Distribution Agreement

In presenting this thesis or dissertation as a partial fulfillment of the requirements for an advanced degree from Emory University, I hereby grant to Emory University and its agents the non-exclusive license to archive, make accessible, and display my thesis or dissertation in whole or in part in all forms of media, now or hereafter known, including display on the world wide web. I understand that I may select some access restrictions as part of the online submission of this thesis or dissertation. I retain all ownership rights to the copyright of the thesis or dissertation. I also retain the right to use in future works (such as articles or books) all or part of this thesis or dissertation.

_____ _____

Julia L Moore Date

The application of degree-day models to study current and future organism development: cautions, limitations, and recommendations

By

Julia L Moore
Master of Science

Graduate Division of Biological and Biomedical Science
Population Biology, Ecology and Evolution

Justin Remais, Ph.D.
Advisor

Berry Brosi, Ph.D.
Committee Member

Lance Waller, Ph.D.
Committee Member

Howie Weiss, Ph.D.
Committee Member

Accepted:

Lisa A. Tedesco, Ph.D.
Dean of the James T. Laney School of Graduate Studies

Date

The application of degree-day models to study current and future organism development: cautions, limitations, and recommendations

By

Julia L Moore
B.A., University of Washington, 2009

Advisor: Justin Remais, Ph.D.

An abstract of
A thesis submitted to the Faculty of the
James T. Laney School of Graduate Studies of Emory University
in partial fulfillment of the requirements for the degree of
Master of Science
in the Graduate Division of Biological and Biomedical Science
Population Biology, Ecology and Evolution
2011

Abstract

The application of degree-day models to study current and future organism development: cautions, limitations, and recommendations

By
Julia L Moore

Degree-day models are mathematical models that have been used extensively to study organism development, particularly in agricultural and public health contexts. Though simple and easy to use, model specifications and parametric uncertainty can influence the results of such applications, often substantially. Yet, model limitations and assumptions are often not considered in the application of degree-day models. This thesis investigates the structural and parametric choices that must be made when using degree-day models, and makes recommendations for how these models can best be applied. First, degree-day model structure and assumptions are comprehensively reviewed. In particular, linear and non-linear developmental functional responses are compared, as are the various methods used to incorporate temperature thresholds and to calculate daily degree-days. Next, uncertainty in two key degree-day model parameters is explored by using a population model of *Oncomelania hupensis*, the intermediate snail host of the parasite that causes schistosomiasis in East Asia, to make predictions of future snail distributions in Sichuan Province, China. I conclude that structural and parametric specifications should be chosen based on the context of the organism under study and the specific temperature patterns of the region. In addition, future predictions of organism distribution are highly sensitive to parametric uncertainty, and thus caution should be used when interpreting the results of degree-day model predictions under scenarios of future climate change. I conclude that, if degree-day model limitations are considered and model assumptions met, degree-day models can be a powerful tool for studying temperature-dependent development.

The application of degree-day models to study current and future organism development: cautions, limitations, and recommendations

By

Julia L Moore
B.A., University of Washington, 2009

Advisor: Justin Remais, Ph.D.

A thesis submitted to the Faculty of the
James T. Laney School of Graduate Studies of Emory University
in partial fulfillment of the requirements for the degree of
Master of Science
in the Graduate Division of Biological and Biomedical Science
Population Biology, Ecology and Evolution
2011

Acknowledgements

Funding for this thesis was provided by an NIH Training Grant in the Population Biology of Infectious Disease, and an NSF Graduate Research Fellowship.

I would like to begin by thanking my research advisor, Dr. Justin Remais, who supported and guided me through lab rotations, conferences in China, and the development and refinement of this work. I would also like to thank my committee members, Drs. Berry Brosi, Lance Waller, and Howie Weiss, for their helpful insights and comments.

Constant support and encouragement was given by my close friends, Alaine B, Geoff M, and Matt R, for whom I will be forever grateful. Additionally, my parents were an unfailing source of guidance and reassurance, without which I never would have made it to this point in my life and in my graduate studies. This wouldn't have been possible without you.

Contents

List of Figures

List of Tables

Introduction

Organism development is typically thought to be a progression through time. Yet, some organisms depend not only on time, but on meeting specific temperature requirements as well. Degree-day models are often used to describe such development, expressing developmental progression as a composite of time and temperature. These models are widely used in agricultural and vector-borne disease contexts, in addition to studies of the potential impact of climate change on such systems. Though widely used and intuitive, degree-day models are subject to limitations and assumptions that are often disregarded. This thesis aims to investigate such limitations and assumptions in order to provide recommendations for situations in which degree-day models can best be applied. The thesis is broken into two parts.

First, in Chapter 1, I review the basic framework of temperature-dependent development models, and compare linear and non-linear developmental functional response forms. I conduct a limited analysis looking at how the choice of different functional responses leads to differences in the predicted time of developmental completion, and discuss the implications of this result for the application of degree-day models. Next, I review various methods of incorporating temperature thresholds and estimating degree-day model parameters. I also review common methods used to calculate daily accumulated degree-days, and perform an analysis

to investigate which methods are more appropriately applied given specific temperature conditions. I conclude Chapter 1 with a discussion on the applicability of degree-day models to study ecological and infectious disease systems, and summarize the general limitations and assumptions that should be accounted for.

In Chapter 2, I investigate the sensitivity of degree-day models to uncertainty in two key models parameters using a population model of *Oncomelania hupensis*, the intermediate snail host of the parasite that causes schistosomiasis in East Asia. With this model, I investigate the sensitivity of mean snail density and time of first population peak to changes in the two model parameters, at both a single spatial location, and across Sichuan Province, China. I conclude this chapter by stressing the importance of interpreting results cautiously when using degree-day models to make predictions of organism responses to climate change.

I conclude with a brief summary of the main results.

CHAPTER 1

Modeling temperature-dependent development: structural, parametric, and experimental issues in degree-day models

1.1. Introduction

Degree-day models are mathematical models that incorporate temperature dependence into developmental processes. Rather than express development as a progression through time, these models describe development as a composite of time and temperature, measured as the cumulative sum of degree-time products, with daily time steps resulting in units of degree-days. Degree-day models have been in use since the 1730s (Reaumur, 1735), and were initially developed for agricultural applications. For instance, agronomists have used these models to estimate optimal times for fertilization and harvest given anticipated temperatures throughout the year (Sharratt et al., 1989), and to estimate the suitability of a given region for specific crops (Ren et al., 2007). Similarly, degree-day models have been used to investigate the impact of specific agricultural practices that affect ambient crop temperature (e.g. the use of plastic film mulches (Diaz-Perez, 2009)), and to predict the timing and intensity of pest infestation, with the goal of determining the optimal time for pesticide application (Dahlsten et al., 1994; Elliott et al., 2009; Nahrung et al., 2008). Degree-day models are so widely used in agriculture and pest management that many local agencies make freely available yearly estimates of

accumulated degree-days for local crops and pests (University of California, 2011a; University of Wisconsin, 2011; University of Illinois, 2011).

Outside of biological applications, degree-day models have been used in the analysis of energy demands of buildings (Buyukalaca et al., 2001), with important applications in the study of the effects of climate on the energy efficiency of various building structures (Tzikopoulos et al., 2005) and energy demand (Christenson et al., 2006). In addition, degree-day models have been used to study the expected annual amount of snowmelt (Semadeni-Davies, 1997), to reconstruct historical climates using glacial evidence (Hughes and Braithwaite, 2008), as well as in forensic studies of decomposition (Dabbs, 2010).

One increasingly popular application of degree-day models is in the study of the effects of climate change on populations of organisms whose distribution and development are highly dependent upon temperature, particularly organisms involved in the maintenance of important human diseases. A common method involves determining the annual degree-days that are required to support current populations, and then, using predicted future temperatures, generate distribution maps of where the annual degree-day requirements are met under future conditions. Statements are then made regarding the future risk or potential for disease transmission. Some examples include the use of degree-day models to study the effects of climate change on malarial mosquito vectors (Lindsay et al., 2010; Yang et al., 2010), the tick vector of Lyme disease (Ogden et al., 2005, 2006), as well as

the intermediate snail host and water-borne life stages of schistosomiasis (Zhou et al., 2008; Yang et al., 2006).

Though simple and easy to use, degree-day model output is sensitive to choices of model structure as well as uncertainties in model parameters. In many cases, these limitations are not considered or discussed when applying degree-day models, potentially leading to conclusions that are invalid. With this in mind, this chapter reviews basic degree-day model formulations and assumptions, and discusses circumstances under which the models are best applied to study ecological systems. First, the basic structure of temperature-dependent development models are described, and common linear and non-linear functional responses are detailed. Next, the statistical and experimental methods used to determine temperature threshold parameters are reviewed, as are the various methods of calculating daily degree-day units. Finally, the limitations of degree-day approaches, with particular cautions for their applications in the study of ecological responses to climate change, are discussed.

1.2. Generalized model of temperature-dependent development

Temperature-dependent development models describe progress towards a developmental target, such as the completion of an instar stage or the onset of reproductive maturation. Let ρ be the rate of development (in units of day^{-1}), where ρ is a function of temperature, T. The gain in development, D, is given by

$$\frac{dD}{dt} = \rho(T). \tag{1.1}$$

The total development that occurs in the interval from time t_1 to t_2 is given by the integral of the rate function (Logan and Powell, 2001; Powell and Logan, 2005). Therefore,

$$D = \int_{t_1}^{t_2} \rho(T(t))dt, \tag{1.2}$$

where D is normalized such that $D = 0$ at the start of development, and $D = 1$ when the developmental target is reached. Since temperature dependence is not uniform over the full range of environmental temperatures, the rate of development can further be expressed as

$$\rho(T) = f(T, \delta_{\min}, \delta_{\text{opt}}, \delta_{\max}), \tag{1.3}$$

where ρ is written in terms of a functional response, f, which is dependent on temperature and three threshold parameters: $\delta_{\min}$, $\delta_{\max}$, and δ_{opt}. Development is limited (i.e. goes to zero) below a lower temperature threshold, $\delta_{\min}$, and above an upper temperature threshold, $\delta_{\max}$. Development is maximized at an optimum temperature, δ_{opt}.

While there are many structural forms available to represent the functional response, most degree-day models express f as a linear function of temperature. The performance of linear and non-linear functional responses varies depending upon the specific shape of the diurnal temperature curve – and thus on regional climate characteristics – in addition to the modeled organisms specific threshold requirements. These issues will be discussed next.

1.3. Developmental functional response

1.3.1. *Linear*

Typical degree-day models express the rate of development as a linear function of temperature, where

$$\rho = \begin{cases} \frac{T}{K} - \frac{\delta_{\min}}{K}, & : \delta_{\min} < T(t) < \delta_{\max} \\ 0 & : \text{else} \end{cases}, \tag{1.4}$$

and thus

$$D(t) = \begin{cases} \int_{t_1}^{t_2} \left[\frac{T(t)}{K} - \frac{\delta_{\min}}{K} \right] dt. & : \delta_{\min} < T(t) < \delta_{\max} \\ 0 & : \text{else} \end{cases}, \tag{1.5}$$

where the optimal threshold, δ_{opt} is generally not included (Figure 1.1; but see Section 1.4). In the linear model, the parameter K is a species- and developmental target-specific parameter that is interpreted biologically as the total number of

degree-day units necessary for development to complete. To see how this interpretation is reached, the linear model can be scaled by multiplying through by K, leading to

$$k = K \cdot D = \int_{t_1}^{t_2} [T(t) - \delta_{\min}]\, dt, \tag{1.6}$$

for all T where $\delta_{\min} < T < \delta_{\max}$. In this expression, k represents the number of degree-day units that are accumulated within a give time interval, and, as described in the previous section, the developmental target is reached once $D = 1$, or when $k = K$. Rescaling the linear model in this way provides a simple expression that intuitively relates the degrees above the minimum threshold to the development that occurs.

The linear model provides a straightforward, accessible method of estimating development rates. However, for many organisms temperature-dependent development is non-linear (Beck, 1983), and treating the response as linear leads to an underestimation of development rates at low temperatures, and an overestimation of development rates at high temperatures (Hilbert and Logan, 1983; Figure 1.1). The linear model is thus best applied when environmental temperatures fall within intermediate temperature ranges for which the linear approximation is valid (Bergant and Trdan, 2006; Bonhomme, 2000). Since it is not unexpected for organisms to experience temperature extremes well outside these intermediate

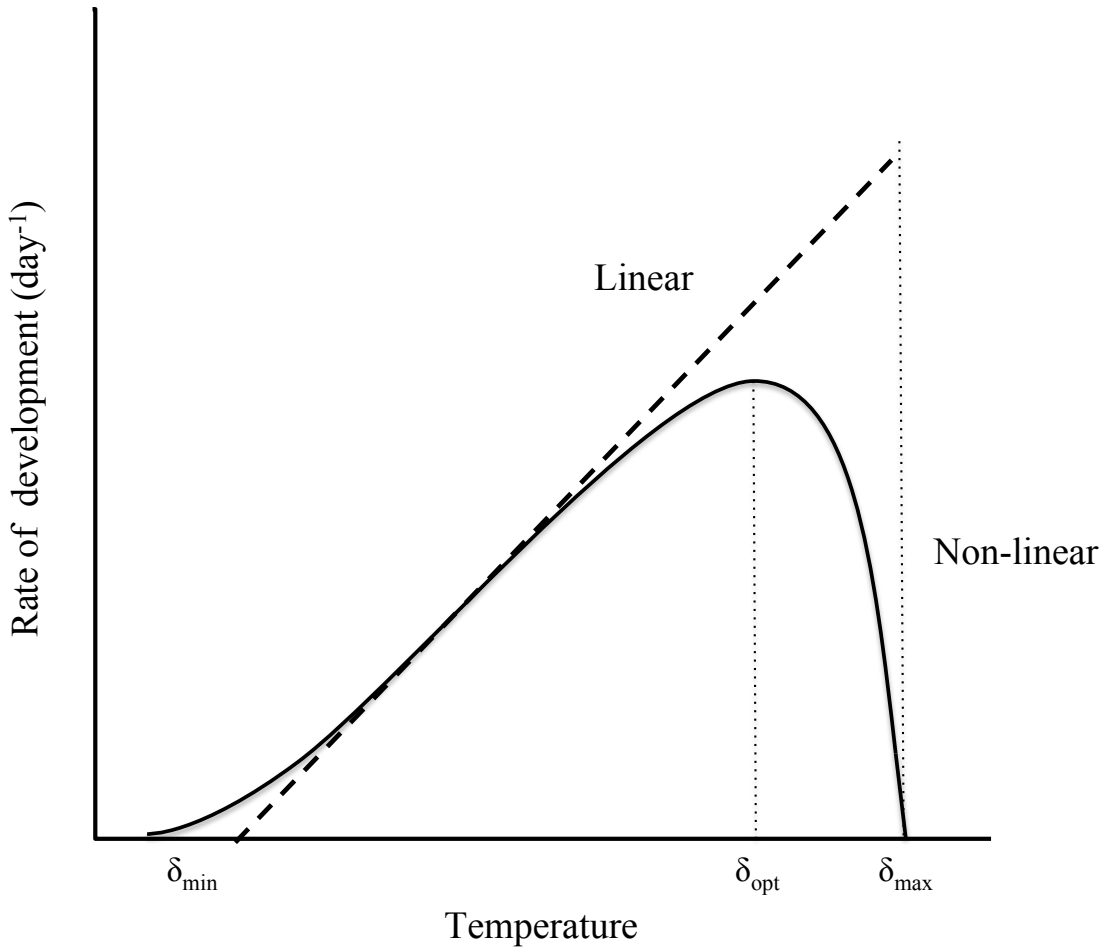

Figure 1.1: *A linear (dashed line) and non-linear (solid line) approximation of the relationship between the rate of development and temperature, and the locations of the three key temperature thresholds,* $\delta_{\min}$*,* δ_{opt}*, and* $\delta_{\max}$*.*

ranges, several non-linear models have been developed as alternative functional forms of f.

1.3.2. *Non-linear*

Several common non-linear models, in addition to the linear model, are shown in Figure 1.2, with model parameters obtained from previous work on *Nephus bisignatus*, a predatory Coleoptera (Kontodimas et al., 2004). It is clear that these

models differ significantly in their behavior at low and high temperatures. The first non-linear model, developed by Sharpe and DeMichele (1977), is based on the biology of enzyme kinetics and provides a mechanistic equation that accurately describes a typical non-linear response at temperature extremes, as well as the linear response at intermediate temperatures. The model is written as

$$\rho = \frac{Te^{((\phi - \frac{\Delta H_A^+}{T})/R)}}{1 + e^{((\Delta S_L - \frac{\Delta H_L}{T})/R)} + e^{((\Delta S_H - \frac{\Delta H_H}{T})/R)}} \tag{1.7}$$

where parameters (Table 1.1) are either physical constants, or organism specific thermodynamic values (Sharpe and DeMichele, 1977).

Though the Sharpe model is able to provide a good fit to data describing the relationship between temperature and development (Hilbert and Logan, 1983), drawbacks to its application include biologically unrealistic symmetry about the optimal temperature that leads to less accurate estimates of development at high temperatures, (Hilbert and Logan, 1983), as well as the large number of parameters that, while biologically meaningful, increase model complexity (Kontodimas et al., 2004).

A second non-linear model that has received considerable attention (Kontodimas et al., 2004), was developed by Logan et al. (1976) and is written as

$$\rho = \psi \cdot \left(e^{rT} - e^{\left(rT_{\max} - \frac{\delta_{\max} - T}{\Delta T} \right)} \right), \tag{1.8}$$

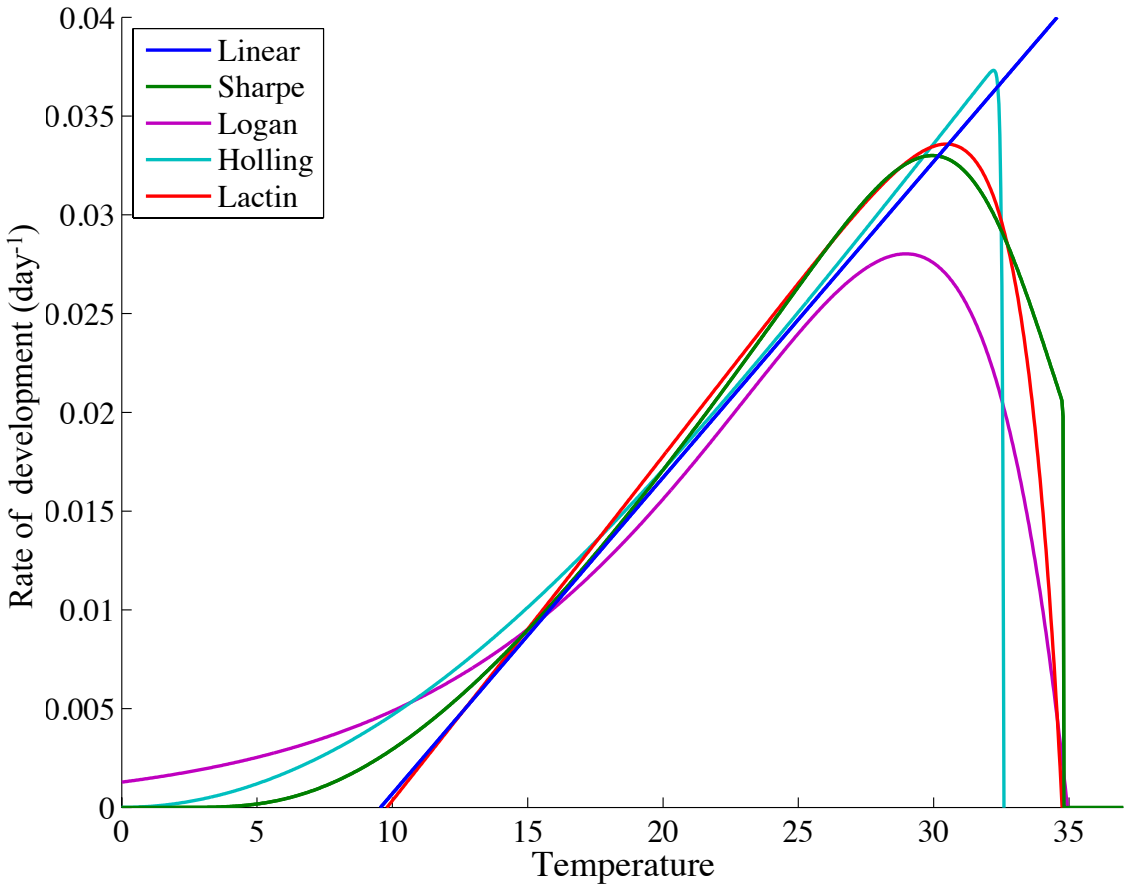

Figure 1.2: *Relationship between temperature and developmental rate for the linear and several common non-linear models.*

where ψ and r are organism specific parameters, and ΔT is equal to the difference between the maximum and optimum temperatures (Table 1.1). Because the Logan model approaches zero asymptotically (Figure 1.2), thus preventing the estimation of $\delta_{\min}$ (Lactin et al., 1995), Hilbert and Logan (1983) derived a new model in which low temperatures were described by a Holling Type III function, allowing estimation of $\delta_{\min}$, with high temperatures described as in the Logan model. This model is

Table 1.1: *Parameters for several non-linear developmental models.*

Parameter	Definition	Reference
Sharpe		Sharpe and DeMichele (1977)
T	Absolute temperature (Kelvin)	
K	Boltzmann constant	
h	Planck's constant	
R	Gas constant	
ϵ_c	Relative enzyme concentration	
$\Delta H_A^{\pm}$	Enthalpy of activation	
ΔH_L	Difference in enthalpy of activation between first inactive state and active state at equilibrium	
ΔH_H	Difference in enthalpy of activation between active state and second inactive state at equilibrium	
$\Delta S_A^{\pm}$	Entropy of activation	
ΔS_L	Difference in entropy of activation between first inactive state and active state at equilibrium	
ΔS_H	Difference in entropy of activation between active state and second inactive state at equilibrium	
ϕ	Simplifying parameter, equal to $\Delta S_A^{\pm} + \ln(\mathrm{K}\epsilon_c/\mathrm{h})$	
Logan		Logan et al. (1976)
T	Air temperature - minimum temperature threshold	
$\delta_{\max}$	Lethal maximum temperature	
ΔT	Difference between $T_{\max}$ and optimal temperature	
ψ	Developmental rate at a given base temperate above the minimum developmental temperature	
r	Rate increase up to optimal temperature	
Holling		Hilbert and Logan (1983)
T	Air temperature - minimum temperature threshold	
$\delta_{\max}$	Lethal maximum temperature	
ΔT	Difference between $\delta_{\max}$ and optimal temperature	
ψ	Developmental rate at a given base temperate above the minimum developmental temperature	
D	Fit parameter	
Lactin		Lactin et al. (1995)
T	Air temperature - minimum temperature threshold	
$\delta_{\max}$	Lethal maximum temperature	
ΔT	Difference between $\delta_{\max}$ and optimal temperature	
r	Rate increase up to optimal temperature	
λ	Fit parameter	

written as

$$\rho = \psi \cdot \left(\frac{T^2}{T^2 + D^2} - e^{\left(\frac{\delta_{\max} - T}{\Delta T}\right)} \right), \tag{1.9}$$

with model parameters described in Table 1.1. Lactin et al. (1995) similarly modified the Logan model to estimate the lower threshold by introducing a

parameter, λ, that forces the equation to intersect the x-axis (Figure 1.2), leading to

$$\rho = e^{rT} - e^{\left(rT_{\max} - \frac{\delta_{\max} - T}{\Delta}\right)} + \lambda. \tag{1.10}$$

In certain systems, the Lactin model has been recommended as one of the best alternatives to the linear functional response due to its ability to accurately fit developmental data, as well as to estimate all three temperature thresholds (Kontodimas et al., 2004; Roy et al., 2002).

A number of other non-linear functional forms of f have been developed, and the reader is referred to Kontodimas et al. (2004) for a review of the merits and limitations of each.

1.3.3. *Comparison of functional response forms*

To see how differences in choice of f influence predictions of development, the linear, Sharpe, Logan, Holling, and Lactin functional responses were used to investigate the emergence times of *Nephus bisignatus*, a predatory Coleoptera distributed throughout Europe. Model parameters were taken from Kontodimas et al. (2004) who fit linear and non-linear models to developmental data from laboratory experiments in which *N. bisignatus* were reared at various constant temperatures. For models that cannot provide estimates of $\delta_{\min}$ or $\delta_{\max}$, the lower and upper rearing temperatures at which no development occurred (10 °C and 35 °C, respectively) were used. Temperature data was obtained from the European

Climate Assessment and Dataset (ECAD, 2011) at hourly increments (from 1 Jan 2003 - 31 Dec 2003) for 16 weather stations in Europe. Stations were chosen to provide a range of yearly temperature profiles, and included 2 stations each from Finland, Germany, Greece, Italy, Netherlands, Sweden, France, and Denmark.

Results across all weather stations were consistent, with the exception that stations in warmer regions yielded an earlier emergence time than those in cooler climates, as expected. Figure 1.3A shows a representative plot of development rates for each of the five models from a weather station in Finland (60.17 °N, 24.95 °E). At temperatures near the lower threshold, the predicted rate of development is greatest for the Holling, Sharpe, and Logan models, and lowest for the linear and Lactin models. This is expected given the shape of the developmental curves at low temperatures (Figure 1.2). At higher temperatures, the Sharpe and Lactin models are essentially equivalent, with both predicting the highest rates of development. As the temperature increases closer to the upper threshold (not shown at this station), the linear model predicts the highest rate of development, while the Holling model decreases drastically. This is expected given the absence of an optimal temperature threshold in the linear model, and the shape of the non-linear models above their optimal thresholds. At intermediate temperatures, all models are approximately equivalent.

Over the course of the season, the Holling model predicts the earliest date of emergence (Figure 1.3B), with the Holling emergence date across all sixteen weather stations on average 8.6 days sooner than predicted by the linear model (95% CI:

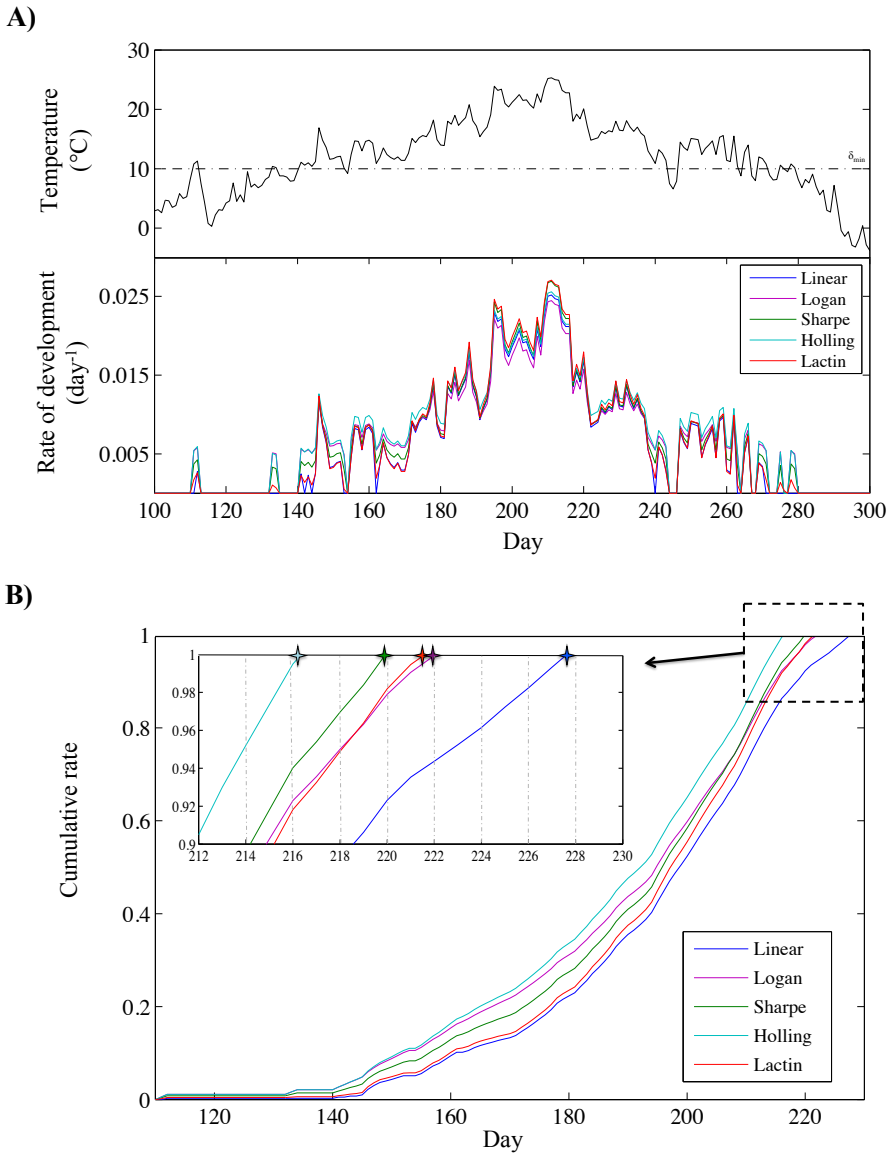

Figure 1.3: *Comparison of the linear functional response and the Sharpe, Logan, Holling, and Lactin non-linear models. A) Daily temperature (top) and developmental rates (bottom) for each of the five models using data from the Finland weather station (see text) from approximately April to October, 2003 (with Day 1 equivalent to Jan 1). Days outside this time range fell below the lower temperature threshold (dotted line in top panel) and thus had a developmental rate equal to zero. B) Cumulative developmental rates for each of the five models showing (in inset) differences in predicted emergence time (when the cumulative rate reaches one) of each model.*

[5.55, 11.58]). The Sharpe, Lactin, and Logan models also predict an emergence time significantly different than the linear model, with emergence dates across all weather stations on average 4.44 days (95% CI: [3.39, 5.48]), 3.75 days (95% CI: [3.01, 4.49]), and 2.81 days (95% CI: [1.64, 3.98]) earlier, respectively.

The differences in predicted emergence time have important implications for the use of degree-day models in ecological applications. For instance, *N. bisignatus* is a predatory insect that is used extensively in the biological control of mealybugs, aphids, whiteflies, and other insect pests (Obrycki and Kring, 1998). When considering biological control measures, the synchrony of developmental timing between the control agent and the pest is known to be important (Corley and Bruzzone, 2009). In the initial selection of biocontrol species, organisms are chosen that are climatically adapted to particular regions, such that the timing of predator emergence coincides with the target life stage of the pest (Samways, 1989). For instance, adult Coleoptera are often released seasonally to augment existing populations, and the timing of this release must be matched to pest populations (Obrycki and Kring, 1998). In addition, many arthropods can complete development in under fifteen days (Danks, 2006). As model predictions differed by up to two weeks, clearly the selection of a functional response for f has important consequences for applications to biological control.

Similarly, selection of a functional response for f is important when examining the potential for disease transmission. Transmission of malaria, for example, is dependent upon the successful development of the parasite within the mosquito

host, a temperature-sensitive developmental process (Beier, 1998), as well as on the probability of the mosquito surviving long enough for parasite development to complete (Killeen et al., 2000). Thus, one crude measure of the potential for malaria transmission in a particular region can be estimated by determining the development time of the parasite and seeing if this falls within the survival time of the mosquito (Paaijmans et al., 2009). Clearly, models producing estimates of parasite development time that differ by several days or even weeks could strongly determine the outcome of such an analysis.

Functional models for f exhibit different behaviors in response to temperature extremes, and thus the functional form chosen should be suitable for both the organism and the climatic conditions under study. Of particular importance given the widespread use of linear degree-day models is that, though simple and intuitive, the response assumes a linear approximation of non-linear development, and thus caution is called for when results are obtained under conditions where temperatures frequently fall outside the linear response range (Bergant and Trdan, 2006). Where this is the case, a non-linear functional response should be considered.

1.4. Temperature thresholds

As discussed in Section 1.2, three important temperature thresholds influence the developmental temperature response. Two thresholds, $\delta_{\min}$ and $\delta_{\max}$, bound the temperature range at which the organism can develop, such that below $\delta_{\min}$ or above $\delta_{\max}$ development ceases, while the third threshold, δ_{opt}, represents the

temperature at which the organism has the highest rate of development. Though $\delta_{\min}$ and $\delta_{\max}$ can easily be specified in the linear model, δ_{opt} is defined only in non-linear models since linear models have no temperature associated with peak development (except as $T \to \delta_{\max}$). To account for the fact that development exhibits diverse behaviors at high temperatures, several threshold cutoff methods have been developed (Roltsch et al., 1999; University of California, 2011b). One method, the vertical cutoff (Figure 1.4A), treats the maximum threshold as previously described, where above $\delta_{\max}$ development ceases. In this method, the optimum temperature threshold is undefined. A second method, the horizontal cutoff (Figure 1.4B), sets the daily temperature to $\delta_{\max}$ when the temperature exceeds the upper threshold. This allows development to continue at a constant rate at all temperatures exceeding the maximum threshold. With the last method, the intermediate cutoff (Figure 1.4C), development proceeds at a decreasing rate as the temperature increases above $\delta_{\max}$. Generally, the development that occurs when $T > \delta_{\max}$ is set equal to $\rho(T) - 2[\rho(T) - \rho(\delta_{\max})]$, which is equivalent to subtracting twice the development that occurs above the maximum threshold from the development that would occur if no upper threshold was considered. Other formulations can be used for intermediate cutoffs to incorporate a steeper or more gradual decline in development rates above $\delta_{\max}$. The intermediate cutoff method is equivalent to treating $\delta_{\max}$ as the optimal temperature, and, though not often done, an additional threshold could then be included above which development ceases

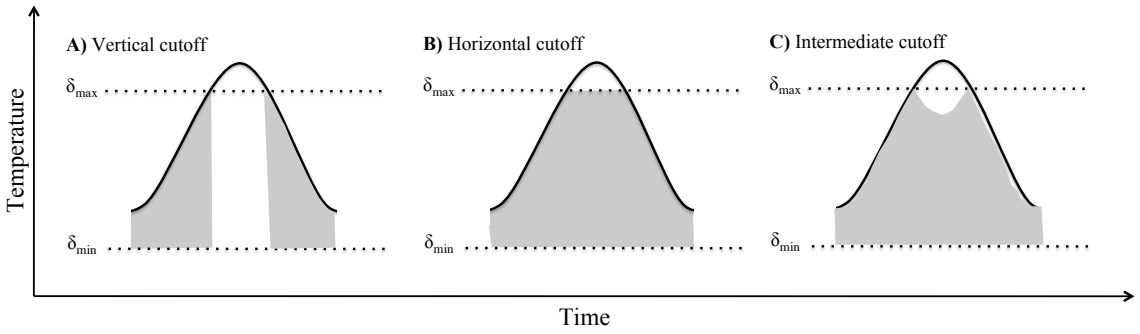

Figure 1.4: *Three common cutoff methods used when calculating daily degree-days. A) vertical cutoff; B) horizontal cutoff; C) intermediate cutoff. Each curve represents the temperature over the course of a single day, while the shaded area indicates the timing and degree of development.*

entirely. Given the diversity of approaches, the cutoff method chosen should reflect the underlying biological response to temperature of the organism under study.

1.4.1. *Estimating temperature thresholds*

Accurate organism-specific parameter values for $\delta_{\min}$, $\delta_{\max}$, and δ_{opt} are crucial, and a variety of methods have been developed to estimate these thresholds experimentally. The most common method used to determine $\delta_{\min}$ is to experimentally derive the temperature-development relationship and then estimate the x-intercept using linear regression (e.g. Campbell et al., 1974; Nahrung et al., 2008; Naves and de Sousa, 2009; Lardeux and Cheffort, 1997). The experiment generally involves determining the number of days, d, required for an organism to develop at a range of constant temperatures. The rate of development, $1/d$, is then regressed on temperature and the x-intercept estimated by solving for the temperature at which the rate is equal to zero. Importantly, due to the high mortality or dormancy commonly experienced at low temperatures (Campbell et al.,

1974), the x-intercept always falls outside the range of experimental temperature, and thus represents an extrapolation of the linear fit (Bergant and Trdan, 2006). Additionally, as described above (Section 1.3.1; Figure 1.1), the non-linearity of most developmental response functions at low temperatures results in an overestimation of $\delta_{\min}$ using linear regression. Extrapolation error and error associated with linearly approximating a non-linear process can lead to significant uncertainties in the estimation of $\delta_{\min}$ (Bergant and Trdan, 2006; Yang et al., 1995). These uncertainties are often disregarded, though methods to quantify the variance and associated confidence intervals for $\delta_{\min}$ are crucial for the accurate application of degree-day models (Campbell et al., 1974; Kontodimas et al., 2004). Importantly, there are also indications that development at constant temperatures differs from development at fluctuating temperatures, and thus care should be taken when applying laboratory-derived estimates to field conditions (Beck, 1983; Brakefield and Mazzotta, 1995; Campbell et al., 1974). A second method to estimate the lower threshold uses iterative techniques in which a range of values for $\delta_{\min}$ are tested against various criteria. These methods are not commonly used, and the reader is referred to Yang et al. (1995) and Snyder et al. (1999) for a detailed discussion of the approach.

To estimate $\delta_{\max}$ and δ_{opt}, non-linear developmental models are used (Kontodimas et al., 2004; Roy et al., 2002). For many non-linear models, these thresholds appear explicitly within the model equation, and thus can be estimated using non-linear regression (e.g. Briere et al., 1999; Sanchez-Ramos and Castanera,

2001; Tobin et al., 2001). With non-linear models in which one or both of these thresholds cannot be directly estimated, $\delta_{\max}$ or δ_{opt} can often be calculated from other model parameters (Roy et al., 2002). For instance, in the Logan, Holling, and Lactin models, $\delta_{\max}$ is explicit in the model, while δ_{opt} is calculated using a second model parameter, ΔT, where $\Delta T = \delta_{\max} - \delta_{\text{opt}}$. An alternative way to determine δ_{opt} is to maximize the non-linear model equation by setting the first derivative equal to zero (Briere et al., 1999; Kontodimas et al., 2004).

1.5. Degree-days

1.5.1. *Estimating the total degree-days required for development,* K

Only linear models can provide a direct estimate of K, the total degree-days required for development, though the above-mentioned drawbacks to linear estimates of $\delta_{\min}$ should be considered when interpreting such results. One method, similar to the x-intercept method used to estimate $\delta_{\min}$, estimates K as the inverse of the slope of the regression line of development rates and temperature (e.g. Bergant and Trdan, 2006; Campbell et al., 1974; Trudgill et al., 2005). A second method uses experimental development data and a known $\delta_{\min}$ to estimate K. A laboratory experiment is conducted in which the organism is grown at a constant temperature, T, and the total degree-days required for development is estimated as $K = d(T - \delta_{\min})$, where d is the number of days required for development (Naves and de Sousa, 2009). Values of K estimated using this method have been shown to

be similar to estimates using the linear regression approach (Naves and de Sousa, 2009).

If experimental data are unavailable, K can be calculated from field data using a known lower threshold, observed development times, and daily temperature data (Lopez et al., 2001). Since daily temperature is not constant, the degree-days accumulated per day, k, are calculated using one of the methods presented in the following section. The summation of the daily accumulated degree-days between the observed beginning and end of development then provides an estimate of K.

1.5.2. *Methods for calculating daily degree-days,* k

The temperature fluctuations that occur throughout the diurnal cycle can greatly influence organism development (Paaijmans et al., 2009), yet records of hourly or finer temporal resolutions are often unavailable, and thus researchers instead rely on daily minimum and maximum temperature data. Several common methods are used to calculate k, the daily degree-days accumulated, using daily minimum and maximum temperatures. These include the daily average method, the triangle and double triangle methods, and the sine and double sine methods (Figure 1.5), all of which assume a linear functional response.

1.5.2.1. *Daily average*

The daily average method (Figure 1.5A) uses daily minimum and maximum temperatures to estimate accumulated degree-days by applying one of two common

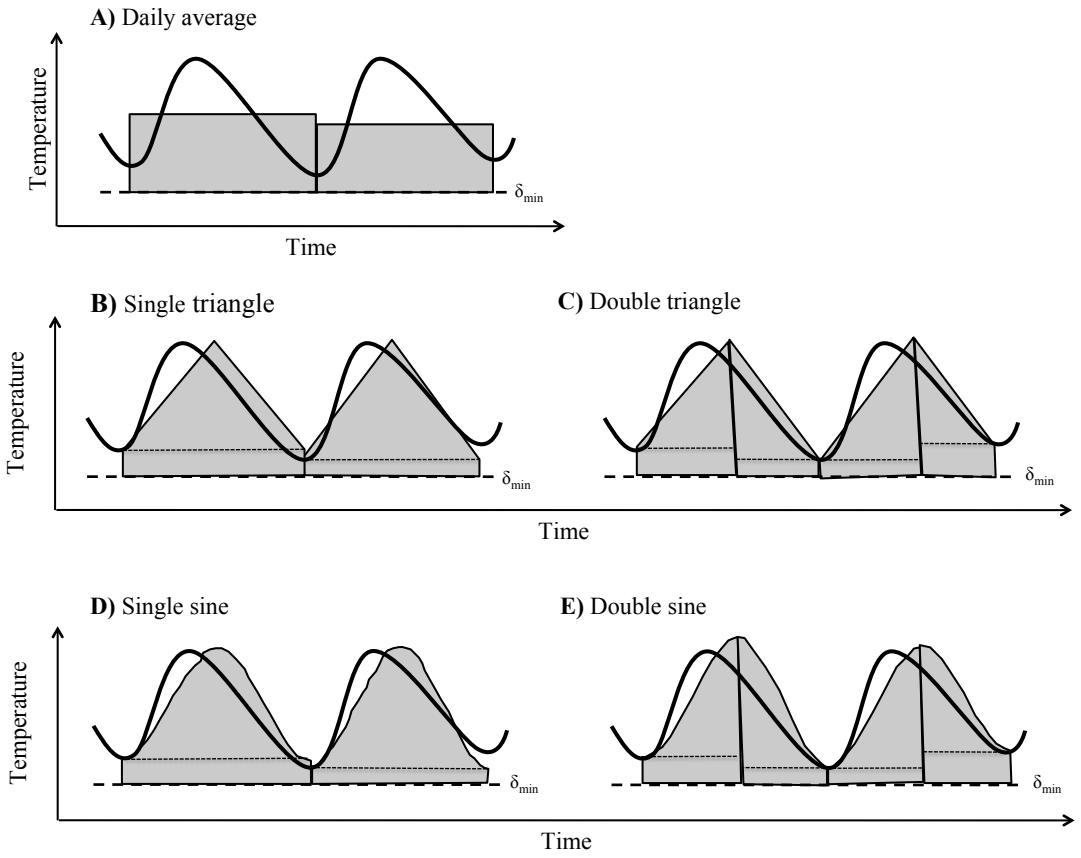

Figure 1.5: *Five common methods used to estimate daily degree-days. Each curve represents the temperature cycle over two days, while the area of the shaded region indicates the degree-days that are accumulated (an approximation to the area under the temperature curve).*

calculations (McMaster and Wilhelm, 1997). The first method finds the average, T_{avg}, of the minimum, T_{min}, and maximum, T_{max}, temperatures and then compares T_{avg} to the lower threshold. The accumulated degree-days is then calculated as

$$k = \begin{cases} T_{\text{avg}} - \delta_{\text{min}}, & : T_{\text{avg}} > \delta_{\text{min}} \\ 0, & : T_{\text{avg}} \leq \delta_{\text{min}} \end{cases} . \tag{1.11}$$

The second method compares the daily minimum temperature to the lower temperature threshold *before* calculating T_{avg}. The accumulated degree-days is then calculated as

$$k = \begin{cases} \frac{T_{\max}+T_{\min}}{2} - \delta_{\min}, & : T_{\min} > \delta_{\min} \\ \frac{T_{\max}+\delta_{\min}}{2} - \delta_{\min}, & : T_{\max} > \delta_{\min} \text{ and } \mathrm{T}_{\min} \leq \delta_{\min} \\ 0, & : \text{else} \end{cases} . \tag{1.12}$$

This ensures that so long as the maximum temperature exceeds $\delta_{\min}$, some degree-days will accumulate.

Despite its simplicity, the daily average method tends to produce surprisingly accurate estimates of the accumulated degree-days when compared to estimates using hourly temperature data (Wilson and Barnett, 1983). However, significant error can result using the first method when the minimum daily temperature drops below the lower threshold, as this often leads to underestimations in the cooler months when the average temperature drops below the minimum threshold, but the maximum daily temperature exceeds the lower threshold (Allsopp and Butler, 1987; Roltsch et al., 1999; Wilson and Barnett, 1983). Additionally, since the average method assumes a symmetrical diurnal temperature profile, error can occur when the shape of the daily temperature curve is skewed such that the maximum temperature occurs closer to either the minimum morning or the minimum evening temperature (Allsopp and Butler, 1987; Wilson and Barnett, 1983).

1.5.2.2. *Triangle and double triangle*

The triangle method estimates the accumulated degree-days by calculating the area under a triangle, with the base of the triangle set at the daily minimum temperature, and the peak at the daily maximum temperature. As implied by the name, the single triangle method (Figure 1.5B) forms a single triangle for each diurnal cycle, while the double triangle method (Figure 1.5C) fits two triangles to each diurnal cycle. With the double triangle method, the base of the first triangle is determined using the minimum temperature of the first half of the day, and the base of the second triangle is determined using the minimum temperature of the second half of the day. Given the minor difference between the two triangle methods, it is perhaps not surprising that they produce similar results (Roltsch et al., 1999).

In the simplest case, both the single and double triangle methods assume a twelve hour difference between when the daily minimum temperature occurs, and when the daily maximum temperature occurs (Allsopp and Butler, 1987; Wilson and Barnett, 1983). This assumption is often modified to better account for the shape of the daily temperature curve by incorporating information on sunrise and sunset times, or solar radiation (Reicosky et al., 1989).

The triangle methods, though still rather simple representations of the daily temperature, can produce results comparable to many of the more complicated methods (Cesaraccio et al., 2001; Roltsch et al., 1999; Reicosky et al., 1989). However, as with the daily average method, significant error in degree-day estimates

typically arise during winter months (Cesaraccio et al., 2001), or when the shape of the temperature curve is skewed (Allsopp and Butler, 1987; Reicosky et al., 1989).

1.5.2.3. *Sine and double sine*

The sine method fits a sinusoid to the interval between the minimum and maximum temperatures. Similar to the triangle methods, the single sine method (Figure 1.5D) fits a single sinusoid to the diurnal cycle, while the double sine method (Figure 1.5E) forms one sinusoid between the morning minimum temperature and the daily maximum, and a second sinusoid between the daily maximum temperature and the evening minimum. Again, similar to the triangle methods, both the single and the double sine waves produce similar results (Roltsch et al., 1999; Wilson and Barnett, 1983). The sine methods typically assume a twelve hour difference between the daily minimum and maximum temperatures, though this has been corrected for in several models (Reicosky et al., 1989). The sine method tends to overestimate degree-days during both the summer (Allsopp and Butler, 1987) and the winter months (Cesaraccio et al., 2001; Roltsch et al., 1999).

1.5.2.4. *Variations*

While the above methods represent the most common approaches used to estimate degree-days, numerous variations have been used. As two examples, Reicosky et al. (1989) explored a variety of techniques using a combination of linear equations, sine waves, and exponential decays, and Cesaraccio et al. (2001) incorporated a square-root function into the double sine method for estimation of

early morning temperatures. Though these methods can potentially produce more accurate estimates of the accumulated degree-days, over the course of several days the results are generally not significantly different from the simpler methods described above (Reicosky et al., 1989; Roltsch et al., 1999).

1.5.3. *Comparison of methods used to calculate* k

The estimate of accumulated degree-days will vary based on the shape of the daily temperature curve (Roltsch et al., 1999; Allsopp and Butler, 1987), the type of upper threshold cutoff used (Roltsch et al., 1999), as well as where the maximum and minimum temperatures fall relative to the upper and lower thresholds (Allsopp and Butler, 1987; Roltsch et al., 1999; Wilson and Barnett, 1983). To demonstrate the sensitivity of k to these factors, accumulated degree-days were estimated using hourly temperature data (from 1 Jan 2007 to 31 Dec 2010) obtained from three US Climate Reference Network (NOAA, 2011) weather stations in the eastern United States (Table 1.2). These stations were chosen to provide a range of yearly temperature profiles across diverse climate zones in the United States, thus providing a diverse set of diurnal temperature shapes, and included stations in northern Maine, western North Carolina, and southwestern Florida. At every station, k for each day across the three year period was calculated from daily minimum and maximum temperatures using the daily average method (Eqn. 1.11), the single triangle method, and single sine method, as well as the horizontal, vertical, and intermediate upper threshold cutoffs. For each day, k was calculated

Table 1.2: *Characteristics of weather stations used to compare methods of calculating daily degree-days. The range of hourly temperatures indicates the maximum and minimum temperatures that occur between 1 Jan 2007 and 31 Dec 2010, while the temperature average is the mean temperature over this time period.*

Location	Latitude	Longitude	Elevation (m)	Range of hourly temperatures (°C)	Average temperature (°C)
Everglades City, Florida	25.9°	-81.318°	1.2	-2.3 – 35.7	22.8
Asheville, North Carolina	35.419°	-82.557°	641	-15.2 – 33.5	12.3
Limestone, Maine	46.96°	-67.883°	224.6	-37.9 – 32.1	4.5

using multiple values for $\delta_{\min}$ and $\delta_{\max}$ in order to examine how the relative difference between daily temperature extremes and the threshold values affected the estimated degree-days. These estimates were then compared to the daily degree-days estimated using hourly temperatures.

Figure 1.6A shows the results using the horizontal cutoff method and assuming a twelve hour difference between the daily minimum and maximum temperatures. The color indicates the difference between the number of degree-days estimated using a given method, and the number of degree-days calculated using hourly data, with a positive value (reds) indicating an overestimation of the particular method, and a negative value (blues) indicating an underestimation. Each of the four quadrants (Q1-Q4) represents different positions of the thresholds relative to the daily minimum and maximum (Figure 1.6B). Cases in which no upper threshold is used are equivalent to the two upper quadrants.

There are distinct differences between the three methods used to calculate k, and these differences are sensitive to the relationship between threshold values and daily temperatures. Both the daily average and the triangle method do well when the daily temperature range falls between the upper and lower thresholds (Q2). The

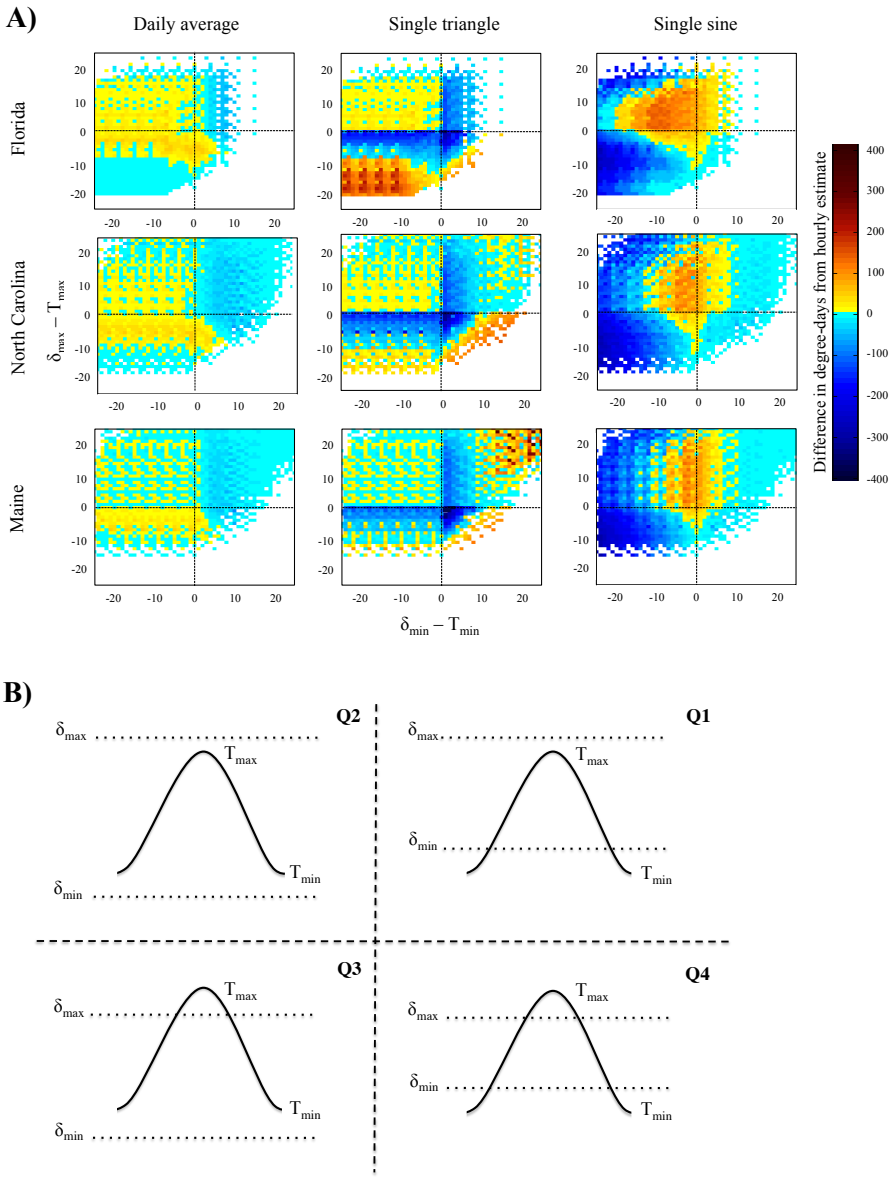

Figure 1.6: *A) Difference between daily degree-days calculated using hourly data, and daily degree-days estimated from the daily average (first column), single triangle (middle column) and single sine (last column) methods, with red colors indicating an overestimation of the particular method, and blue colors indicating an underestimation. For each plot, the color at every point represents the average difference in degree-days for each day of the time series that meets the specified distance between the minimum and maximum daily temperature ($T_{\min}$ and $T_{\max}$) and the lower and upper thresholds, respectively, with distances from the lower threshold given along the x-axis, and distances from the upper threshold given along the y-axis. B) Relative positions of the daily minimum and maximum temperatures to the lower and upper thresholds. Each curve represents the temperature cycle for a single day.*

sine method, in contrast, tends to overestimate the degree-days in this region, particularly when $\delta_{\min}$ is close to the daily minimum temperature. If a similar plot is made that corrects for the time between the daily minimum and maximum temperatures, rather than assuming a twelve hour difference (data not shown), this overestimation is greatly reduced, indicating that the estimate is sensitive to the shape of the temperature curve. This overestimation from the sine method is also present (and can be corrected for) when $\delta_{\min}$ is greater than, though still close to, the daily minimum temperature (Q1). Both the daily average and the triangle methods produce an underestimation in this region, with the exception of the triangle method in Maine, which produces overestimations when there are large differences between $\delta_{\min}$ and the daily minimum. As discussed in Section 1.5.2.1, this underestimation of the daily average method is a result of averaging the daily minimum and maximum temperatures before the comparison with $\delta_{\min}$.

When both $\delta_{\min}$ and $\delta_{\max}$ fall within the daily temperature range (Q4), the sine and daily average method behave similarly, producing slight underestimations in the number of degree-days. The triangle method, in contrast, more severely underestimates the degree-days when $\delta_{\min}$ and $\delta_{\max}$ are both near the daily minimum and daily maximum temperatures, respectively. However, as the difference between $\delta_{\min}$ and $\delta_{\max}$ decreases, the triangle method begins to overestimate the degree-days.

When $\delta_{\min}$ is less than the daily minimum temperature and $\delta_{\max}$ is less than the daily maximum temperature (Q3), the average method overestimates the degree-days when $\delta_{\max}$ is near the maximum temperature. The sine method

produces underestimates in this region, while the triangle method produces underestimates when $\delta_{\max}$ is near the daily maximum and overestimates as $\delta_{\max}$ drops far below the daily maximum. Again, this overestimation with the triangle method is significantly reduced when the time between the daily minimum and maximum temperatures is corrected for, indicating that this overestimation is sensitive to the shape of the diurnal temperature cycle.

In summary, the daily average method generally provides accurate estimates of daily degree-days, with the exception of overestimates when $\delta_{\max}$ and $\delta_{\min}$ drop below the daily maximum and minimum temperatures, respectively, and underestimates when $\delta_{\max}$ and $\delta_{\min}$ fall above the daily maximum and minimum temperatures, respectively. The triangle method performs well when the daily temperature range falls within both threshold values. In the other regions, the triangle method tends to either over or underestimate the daily degree-days. Finally, the sine method tends to underestimate the daily degree-days, with the exception of regions where $\delta_{\max}$ exceeds the daily maximum temperature and $\delta_{\min}$ is close to the daily minimum temperature.

Comparing the different geographic regions indicates that the shape of the diurnal temperature curve, which changes with latitude and elevation, affects the accuracy of the estimation methods. For instance, when the minimum and maximum thresholds are less than the daily minimum and maximum temperatures, respectively (Q3), the triangle method tends to overestimate the degree-days in Florida, while tending to underestimate the degree-days in Maine. This result is

also observed with the sine method when the temperature range falls within both thresholds (Q2). Since the relative difference between the daily temperature extremes and the threshold values is the same between the regions, the shape of the diurnal temperature cycle is clearly responsible for this effect.

If a vertical threshold cutoff is used rather than a horizontal cutoff, the results are similar with only a few differences (data not shown). First, the vertical cutoff improves performance of the triangle and sine methods when both thresholds fall within the daily temperature range (Q4), whereas the daily average method tends to overestimate the degree-days in this region. When $\delta_{\min}$ and $\delta_{\max}$ are both less than daily minimum and maximum temperatures, respectively (Q3), the performance of the sine method improves, while the triangle method now significantly overestimates the degree-days. Importantly, where the daily average method produced overestimates in Q4 using the horizontal cutoff, the vertical cutoff exacerbates this overestimation. When $\delta_{\max}$ exceeds the daily maximum temperature (Q1 and Q2), there is no change in the performance of the methods, as no cutoff is ever applied. Similar results are observed using the intermediate threshold cutoff, with the effects of the underestimation more pronounced.

It is apparent that there are many factors that affect the accurate estimation of daily degree-days, and the results presented here indicate than no one method is universally superior to another, but rather each exhibits behaviors sensitive to where the thresholds fall relative to the daily minimum and maximum temperatures, the type of cutoff used, as well as the shape of the daily temperature

Table 1.3: *A summary of the performance of the daily average, single triangle, and single sine methods used to calculate degree-days, given different relative positions of the thresholds and the daily temperature extremes (with table quadrants corresponding to quadrants Q1-Q4 in Figure 1.6B). Methods shown in bold indicate the best method for the given quadrant.*

$\delta_{max} > T_{max}$, $\delta_{min} < T_{min}$ (Q2)	$\delta_{max} > T_{max}$, $\delta_{min} > T_{min}$ (Q1)
Average: generally accurate	**Average: slight underestimates**
Triangle: generally accurate	Triangle: strong underestimates, strong overestimates
Sine: strong underestimates, strong overestimates	**Sine: slight underestimates**, (strong overestimates when δ_{min} close to T_{min})
$\delta_{max} < T_{max}$, $\delta_{min} < T_{min}$ (Q3)	$\delta_{max} < T_{max}$, $\delta_{min} > T_{min}$ (Q4)
Average: generally accurate, (slight overestimates when δ_{max} close to T_{max})	Average: slight underestimates, slight overestimates
Triangle: strong underestimates, strong overestimates	Triangle: strong underestimates, strong overestimates
Sine: strong underestimates	**Sine: slight underestimates**

curve (as implied by differences between regional zones). Table 1.3 summarizes the performance of the various methods and indicates the method(s) that are likely the most appropriate given the relative positions of the thresholds. Importantly, this analysis only considers error on a daily basis; these errors might be amplified, or might cancel out, over the course of an entire season or year, depending on the frequency with which daily temperature profiles land in each of the quadrants.

1.6. Discussion

Degree-day models are useful tools for analyzing the temperature-dependent development of organisms important for agriculture and infectious disease transmission, among other applications. By assuming a linear response to temperature and relying on a minimal number of parameters that can be estimated

through simple growth experiments, these models are straightforward to apply and are thus accessible to a wide variety of researchers.

Degree-day models, however, have key limitations when used to estimate when specific development targets will be reached, or the temperature suitability of a given region for specific organisms. Temperature is unquestionably important in the developmental processes of many organisms, but both linear and non-linear models may be insufficient for representing the complete effects of temperature on an organism. For instance, though organisms may continue to develop at the extremes of their temperature range, stress sustained at these temperatures can have important implications. For example, in agriculture, heat stress can lead to diminished crop quality or yield (Thakur et al., 2010); in a public health context, temperature can also influence vector competence or host immunity (Kilpatrick et al., 2010; Bensadia et al., 2006). Additionally, temperature is not the only factor that influences development, as organisms are also dependent upon the availability of sufficient resources (Campbell et al., 1974; Hagstrum and Milliken, 1988; Logan et al., 2007), are affected by numerous environmental conditions (e.g. humidity, precipitation) (Hagstrum and Milliken, 1988), and interact with their surrounding biotic and abiotic environment (Logan et al., 2007). Thus, establishing that the necessary temperature requirements for development are met is not likely sufficient for assessing the viability or establishment of an organism in a particular region or climate.

Caution, then, is needed when applying degree-day models to questions regarding species' range expansions or contractions in response to climate change (e.g. Lindsay et al. (2010); Zhou et al. (2008)). First, the degree-day model should not be applied to future climates that fall outside the temperature range for which the model was parameterized. Second, temperature may interact with other climate-mediated ecological changes (e.g. changes in predator densities), and therefore incorporating degree-day models into dynamical population models that account for relevant biotic interactions offers promise (Kingsolver, 1989). Anthropogenic impacts, such as habitat degradation or altered land use, can also interact with temperature to produce novel effects that can be understood by dynamical models in combination with the degree-day framework.

Importantly, degree-day models assume constant threshold values, even when applied to questions posed over long time scales, such as in studies of future climate change. It is well established, however, that populations can adapt to local conditions, as evidenced by species in more temperate regions, for example, having a lower temperature threshold than those in the tropics (Trudgill et al., 2005). This implies that minimum, maximum, and optimum temperatures determined for organismal development today may not be valid under future conditions. This is especially important when studying coupled organisms, such as consumer-resource pairs (Logan, 2007). Parasites, for instance, often have a higher temperature threshold than their hosts, ensuring that host development is completed before the parasite becomes viable (Campbell et al., 1974). If the temperature thresholds, or

the shape of the temperature-development response for either organism changes, it is possible that this synchrony might be disrupted. This has important implications, not only for disease systems, but also for the persistence and distribution of other coupled organisms, such as plants and their pollinators, or predators and their prey (Visser and Both, 2005).

A major limitation to improving degree-day model applications is obtaining suitable temperature data. Often, mean monthly temperatures (e.g. Craig et al., 1999; Yang et al., 2006) are used to calculate degree-days, yet even daily temperature fluctuations can have significant effects on organism development, as well on disease transmission (Paaijmans et al., 2009, 2010a). Thus daily, or even hourly, temperature data should be used whenever available. In addition, careful consideration should be given to the location at which the temperature is measured. In some cases, micro-environmental temperature, such as soil temperature (Zhang et al., 2008), or water temperature (Paaijmans et al., 2010b), rather than ambient air temperature, might better represent the conditions experienced by the organism. Finally, the distance between the station where the weather is collected and the population under study also influences the reliability of the temperature data (Dabbs, 2010). Though these limitations are important to consider, often researchers are constrained by the availability of site-specific temperature data collected at sufficiently short increments. In these cases, model predictions should be interpreted cautiously.

The degree-day model provides a simple and effective means of describing and estimating temperature-dependent development of a diverse set of organisms. Attention paid to meeting the assumptions of the approach and recognizing its limitations can yield models that provide considerable insight into questions of organism distribution, emergence times, and the effect of environmental change.

CHAPTER 2

Cautioning the use of degree-day models for climate change projections: predicting the future distribution of parasite hosts in the presence of parametric uncertainty

2.1. Introduction

Research that quantitatively examines the relationship between climate and patterns of diseases carried by vectors or intermediate hosts often relies on degree-day models, mathematical models that incorporate temperature dependence into developmental processes. Degree-day models express the temperature and time requirements for development in units of degree-days, which accumulate only when the temperature exceeds a minimum threshold. Degree-day models have been used since the early 18th century (Reaumur, 1735) to study plant and pest development in agriculture, and are increasingly being applied, either singly or coupled with population dynamics modeling, to study the effects of climate change on organisms associated with important human infectious disease. For this application, degree-day models are often used to predict changes in the geographic distribution of vectors, intermediate hosts, or pathogens under future climate conditions. Table 2.1 lists recent examples, with a description of the structural and parametric choices that were made in each case.

Table 2.1: *Applications of degree-day models to predict vector or intermediate host responses to climate change.*

Disease: Vector	Environmental variable(s)	Temperature data	Temperature thresholds	Model type	Citation
Malaria: *Anopheles* species	temperature	mean daily	minimum developmental temperature	biology-based model	Lindsay et al. (2010)
	temperature, rainfall, humidity	mean daily	minimum developmental temperature	biology-based and statistical model	Yang et al. (2010)
Schistosomiasis: *Oncomelania hupensis*	temperature	mean daily	minimum developmental temperature, minimum lethal temperature, maximum lethal temperature	biology-based model	Zhou et al. (2008)
	temperature	mean monthly	minimum developmental temperature	time-series	Yang et al. (2006)
Lyme disease: *Ixodes scapularis*	temperature	mean monthly	minimum developmental temperature	biology-based model	Ogden et al. (2005, 2006)
Leishmaniasis: *Lutzomyia longipalpis*	temperature, surface/soil moisture	mean monthly	minimum developmental temperature	growing degree-day water-budget model	Nieto et al. (2006)
West nile virus: *Culex pipiens*	temperature	daily minimum and maximum	minimum developmental temperature	GIS degree-day model	Zou et al. (2007)

The degree-day model can be expressed as

$$D = \int_{t_1}^{t_2} \left(\frac{T(t)}{K} - \frac{\delta_{\min}}{K} \right) dt, \tag{2.1}$$

for $\delta_{\min} < T(t) < \delta_{\max}$, where D is the development that occurs in the interval from time t_1 to t_2, $T(t)$ is the temperature at time t, $\delta_{\min}$ is the lower temperature threshold, below which no development occurs, and $\delta_{\max}$ is the upper temperature threshold, above which no development occurs. Development begins when $D = 0$

and ends when $D = 1$. The parameter K is interpreted biologically as the total degree-days necessary for the completion of development. This interpretation becomes clear if Eqn. 2.1 is rescaled such that

$$k = K \cdot D = \int_{t_1}^{t_2} (T(t) - \delta_{\min})\, dt, \tag{2.2}$$

where k represents the number of degree-day units that accumulate in the given interval. In this equation, the onset of development occurs when $k = 0$, and completes when $D = 1$, or, equivalently, when k equals K degree-days. Depending on model implementation and the biology of the organism under study, additional model parameters can be incorporated, such as optimal and lethal temperature thresholds.

Considerable uncertainty exists in the estimation of degree-day model parameters. Typically, estimates of $\delta_{\min}$ and K are obtained experimentally by measuring the rate of organismal development under a range of constant temperatures. A linear function is then fit to these data and extrapolated, often considerably, outside the experimental temperature range to determine both the minimum temperature at which development can proceed, $\delta_{\min}$, as well as the total number of degree-days necessary for development to complete, K (Campbell et al., 1974). Uncertainty due to measurement error, as well as the extrapolation procedure, can lead to significant challenges in generating accurate parameter estimates (Bergant and Trdan, 2006). As an example, Kontodimas et al. (2004)

calculated $\delta_{\min}$ and K for a predatory beetle, *Nephus bisignatus*, as 9.39 °C (95% CI: [8.31, 10.46]) and 614.25 degree-days (95% CI: [563.96, 664.54]), respectively. Similarly, Nahrung et al. (2008) calculated $\delta_{\min}$ and K for an immature life stage of *Paropsis atomaria*, a pest of eucalypt plantations, as 5.4 °C (95% CI: [-0.28, 11.08]) and 166.7 degree-days (95% CI: [114.17, 219.23]), respectively. These confidence intervals are sizable, and such wide variance may have a substantial impact on predictions of organism emergence times, or in determining the suitability of specific regions for organism establishment or persistence.

In applications of degree-day models to study a species' response to future climates the effects of variance in model parameters are rarely considered; even when confidence intervals are available from previous work, point estimates of parameters are often borrowed directly from the literature for use in such analyses, with the influence of parametric uncertainty remaining unexplored (e.g. Lindsay et al., 2010; Yang et al., 2006, 2010). Thus, while degree-day models provide a simple, easy tool for making predictions of how infectious disease systems may respond to climate change, there has been limited critical assessment of whether these models are sufficiently robust to inform public health planning and decision-making. Here, the implications of uncertainty in degree-day model parameters are explored through a developmental model of *Oncomelania hupensis*, the intermediate snail host of the parasite that causes schistosomiasis in East Asia. The model is used to generate predictions of *O. hupensis* distribution in Sichuan Province, People's Republic of China (PRC), under future climate conditions. Note

that the purpose is not to develop the definitive model for estimating the distribution of *O. hupensis* in future climatic conditions, but rather to examine the influence of parametric uncertainty on the output of a plausible model. The sensitivity of 1) model-predicted *O. hupensis* density at selected locations within Sichuan, and 2) model-predicted geographic distributions of *O. hupensis*, is explored with respect to changes in the two key model parameters, $\delta_{\min}$ and K. The results are then discussed in the context of the suitability of degree-day models for examining ecological responses to climate change.

2.2. Materials and methods

The analysis was structured as follows. First, a temperature-dependent population model for *O. hupensis* was developed to simulate current and future snail populations. Temperature datasets generated for both contemporary and future conditions served as model inputs, and to ensure biological plausibility, the model was fit to historical data on the distribution of *O. hupensis* in Sichuan Province. Finally, to investigate the influence of uncertainty in $\delta_{\min}$ and K, a sensitivity analysis was conducted at selected locations within Sichuan, as well as on the predicted future distribution of *O. hupensis* across Sichuan. The following sections detail each of these steps.

2.2.1. *Population model*

Schistosoma japonicum, the intestinal trematode that causes schistosomiasis, infects more than 700,000 people in China (Zhou et al., 2007). The presence of the intermediate snail host, *Oncomelania hupensis*, is required for transmission to humans and other mammals (Ross et al., 2001), and thus the geographic distribution of the snail restricts transmission in China. In Sichuan Province, *O. hupensis* inhabits irrigation canals and terraces, and environmental factors such as humidity, precipitation, and temperature are all important for snail survival and reproduction (Ross et al., 2001). Temperature is an especially important variable, and models used to describe the population dynamics and geographic range of *O. hupensis* frequently include the influence of temperature using degree-day formulations (Liang et al., 2002, 2005; Remais et al., 2007; Zhou et al., 2008).

Here, a temperature-dependent, dynamic *O.hupensis* population model was adapted from previous work (Liang et al., 2002), and is expressed as a delay differential equation given by

$$\frac{dS}{dt} = \sum_{\lambda \in N_t} \left[e^{-\lambda\mu} e^{[-\alpha S_{t-\lambda}]} \beta e^{[-\kappa (T_{t-\lambda} - \delta_{\text{opt}})^2]} S_{t-\lambda} \right] - \mu S_t, \tag{2.3}$$

where S is the snail density, μ is the snail mortality rate, $T_{t-\lambda}$ is the temperature at time $(t-\lambda)$, and the summation represents the total number of snails that complete development at time t. The value within the summation is determined by the recruitment of snails at time $(t-\lambda)$, given by $\beta e^{[-\kappa (T_{t-\lambda} - \delta_{\text{opt}})^2]} S_{t-\lambda}$, reduced by a

Table 2.2: *Parameters for the O. hupensis population model, with ranges obtained from Liang et al. (2005).*

Parameter	Definition	Range
S_0	Initial snail density (per Kuang [1 Kuang = 0.11 m^2])	17-35
μ	Snail mortality rate (per day)	0.0023-0.007
β	Maximum snail reproduction rate (per day)	0.01 -2
α	Density dependence	0.001-0.3
κ	Recruitment kurtosis	1-5.2
δ_{opt}	Optimum reproduction temperature (°C)	20-25
δ_{min}	Minimum temperature threshold for development (°C)	7-12
K	Total degree-days required for completion of snail development	1200-1500
λ	Time delay	varies

density dependent factor, $e^{[-\alpha S_{t-\lambda}]}$, and by mortality that occurs between snail birth and the completion of development, $e^{-\lambda\mu}$. N_t is the set containing all time points prior to time t for which $\int_{t-\lambda}^{t}(T(t) - \delta_{\min})dt = K$. That is, N_t represents the set of all delays, λ, for which the snails born at time $(t - \lambda)$ complete development at time t. Under certain temperature conditions, snails born at different time steps can complete development on the same time step.

Mean daily temperature is used here, as in other models (Table 2.1), but see Chapter 1 and Paaijmans et al. (2009, 2010a) for a discussion on the implications of using daily vs. hourly temperature data. The daily average method of calculating daily degree-days (Wilson and Barnett, 1983) was used, and no upper threshold was incorporated. Definitions for individual parameters in Eqn. 2.3 are given in Table 2.2.

2.2.2. *Temperature data*

To generate a surface of contemporary and future daily temperature values for Sichuan Province, mean daily temperature data from 1 Jan 1980 to 31 Dec 2009

were obtained from the National Oceanic and Atmospheric Administration National Climatic Data Center (NOAA, 2011) for 68 weather stations located within a rectangular region (longitude 97.933 °W and 104.73 °W, latitude 26.367 °N and 34.1 °N) encompassing Sichuan Province. Mean daily temperature in these datasets were reported in °F and were derived from a minimum of four observations per day. All weather stations within a 200 km buffer distance around the boundary of Sichuan province were selected so as to ensure accurate temperature interpolation at border regions. Only those weather stations reporting daily mean temperature for more than three years between 1980 and 2009 were included. Weather station locations were geo-coded to Sichuan Province using ArcGIS (version 9.2) and overlaid on a digital elevation model (DEM) of the region. Geospatial modeling, described below, was conducted using Spatial Analyst in ArcGIS (version 9.3).

From the station data, an interpolated contemporary temperature dataset was generated at a grid of 90 by 90 meter cells across Sichuan Province as follows. First, mean daily temperature values for each station were averaged on each day of the year over all years between 1980 and 2009 for which data were reported. This produced a single year of averaged daily temperature data at each station (366 days of data, as a consequence of leap years). To interpolate these daily temperatures across every grid cell in Sichuan, a multiple linear regression model was constructed that predicts daily temperature from elevation, latitude and longitude variables following methods described elsewhere (Chuanyan et al., 2005). A separate model was fit for each day using data from all stations, with modeling carried out

iteratively using the R statistical package (version 2.7.1). Regression coefficients for each of the 366 days were then used to predict a mean daily temperature at each 90 by 90 meter cell across the full spatial domain, yielding a contemporary temperature dataset consisting of 366 surfaces, each representing one day of interpolated mean temperature.

To generate a future temperature dataset for 2050, the original temperature data for all 68 weather stations were entered into a statistical model that incorporates latitude, elevation, and time variables. The resulting future temperature projection makes the simple assumption that the rate of temperature increase observed between 1980 and 2009 in Sichuan will continue unchanged into the future. First, daily mean temperature data from 1980 to 2009 was averaged at each station to provide monthly means. A mixed-effects model was constructed to fit mean monthly temperature to elevation, latitude, longitude, and seasonal variables (Table 2.3) using the STATA function for cross-sectional time-series analysis, *xtgee*, and weather station as the panel variable. An F-test was used to compare a reduced model to the full model, and the final model was selected by evaluating the accuracy of predictions in a data-splitting procedure, using the first 10 years of temperature data to predict the last 20 years of data, and using the first 20 years of temperature data to predict the last 10 years of data. The final model was also evaluated by comparing model predictions to the 2050 Intergovernmental Panel on Climate Change (IPCC) estimates of seasonal temperature in western China (Solomon et al., 2007). The selected model was applied at every 90 by 90 meter cell of the spatial

Table 2.3: *Predictor variables tested for significance in the statistical temperature projection model, resulting p-values in the full and final models, and variable coefficients included in the final model.*

Variable	Description	p-values		Coefficients
		Full model	*Final model*	*Final model*
s	Station number, equal to 1–68			
m	Month in series, beginning with Jan 1980 = 1			
mc	Month in series centered, equal to $m - m_{avg}$	0.000	0.000	0.006
mc^2	Month in series centered, squared	0.008	0.023	0.000012
x	Latitude	0.250	0.000	-1.174
y	Longitude	0.555	—	—
z	Elevation (meters)	0.000	0.000	-0.007
x^2	Latitude, squared	0.591	—	—
y^2	Longitude, squared	0.444	—	—
xy	Cross-product of latitude and longitude	0.330	—	—
cos_1	$cos(\frac{m\pi}{6})$	0.000	0.000	-13.221
cos_2	$cos(\frac{2m\pi}{6})$	0.000	0.000	-1.425
cos_3	$cos(\frac{3m\pi}{6})$	0.022	0.022	-0.241
cos_4	$cos(\frac{4m\pi}{6})$	0.018	0.018	-0.132
sin_1	$sin(\frac{m\pi}{6})$	0.000	0.000	-7.249
sin_2	$sin(\frac{2m\pi}{6})$	0.000	0.000	-0.584
sin_3	$sin(\frac{3m\pi}{6})$	0.003	0.003	-0.191
sin_4	$sin(\frac{4m\pi}{6})$	0.007	0.008	-0.081

domain using the associated predictor variables, with the month in series variable (Table 2.3) projected forward to 2050 to yield a one year time-series of monthly temperature. The resulting monthly temperature dataset was linearly interpolated to yield a daily temperature value at each cell for 2050. For both contemporary and future datasets, all temperatures were converted to °C, and the 366 days of daily temperature were looped to provide three years of simulation input.

2.2.3. *Parameter estimation using historical* Oncomelania hupensis *presence in Sichuan Province*

Using the parameter ranges in Table 2.2 as a starting point, the dynamic population model (Eqn. 2.3) was fit to the historical distribution of *O. hupensis* to generate a final set of parameter values for use in the sensitivity analysis (Section

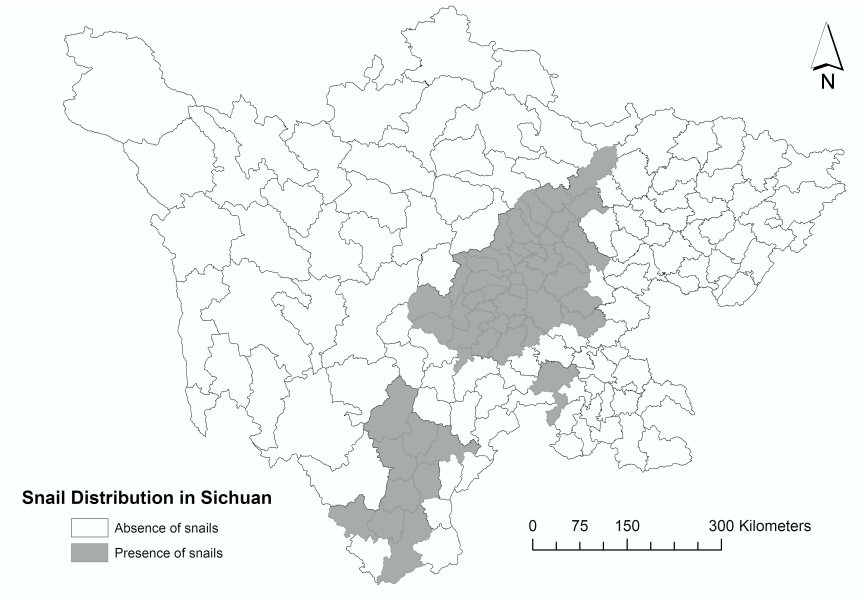

Figure 2.1: *County level data of historical Oncomelania hupensis presence (shaded regions) and absence (white regions) in Sichuan Province.*

2.2.4). Historical data on the presence and absence of *O. hupensis* between 1950-1970 was obtained from routine surveys conducted bi-annually (April-May, September-October) at 63 anti-schistosomiasis stations located throughout counties in Sichuan Province (Ministry of Health, 1992; Qian, 1987). The data was aggregated such that if any life stage of *O. hupensis* was observed (e.g. egg, juvenile, or adult) at any time within the range of dates examined, the county in which the snail was observed was marked as a presence. This method leads to a conservative estimate of snail presence (Figure 2.1), and is intended to approximate the natural range of *O. hupensis* while being robust to the decades of snail control measures conducted in the region (Wang et al., 2009).

To narrow the parametric values from the starting ranges given in Table 2.2, the model in Eqn. 2.3 was fit to the historic *O. hupensis* presence/absence data as

follows. First, to reduce computation time, a subset (n=365) of the total number of cells within the spatial grid was chosen at equal intervals within counties in central and eastern Sichuan, with the number of cells per county proportional to county size. At each cell of the subset, a total of 2000 simulations of Eqn. 2.3 were run using the contemporary temperature dataset as input and parameter values drawn randomly from the ranges in Table 2.2. The minimum snail density over the three years of simulation time was found at every cell of the subset for each simulation, and this minimum was used to generate a threshold snail density, $s_{\min}$, such that agreement between cells classified as present (minimum snail density $> s_{\min}$) or absent (minimum snail density $< s_{\min}$) and the historical distribution described above was maximized. Simultaneously, simulation performance (i.e. agreement with historical distribution) was evaluated with respect to parameter values drawn. Thus, the constraint on model output provided by the historical distribution data was used to reduce parametric uncertainty, treating the threshold density for "presence" as a parameter, in addition to those listed in Table 2.2.

A full exploration of the multi-dimensional parameter space across the entire spatial domain is computationally prohibitive, and, what is more, the goal is simply to produce a plausible population model (and associated parameter values) that agrees generally with observations, not to produce a definitive method of predicting *O. hupensis* distribution in Sichuan. Thus, parameter sets were selected for use in the sensitivity analysis when the following four criteria were met: 1) the agreement between simulated presence and historical presence was greater than 50%; 2) the

agreement between simulated absence and historical absence was greater than 60%; 3) the total agreement between simulated data and historical data was greater than 60%; 4) the agreement at selected locations with specific regional characteristics was greater than 80%. These rather flexible criteria allowed parameters to be selected even when fitting the model to the coarse historical data using only temperature as a predictive variable. Indeed, higher agreement between simulations and historical data is not expected. For the fourth criteria, three counties in mountainous regions (n=31 cells) and three counties in the warmer, low-lying regions of the Province (n=9 cells) were chosen to ensure that selected parameter sets yield output that is regionally consistent.

2.2.4. *Sensitivity analysis*

To explore the implications of degree-day model parametric uncertainty, an analysis of the sensitivity of model output to uncertainty in $\delta_{\min}$ and K was carried out at two scales. First, uncertainty was explored intensively at individual locations (n=6) within Sichuan Province, examining changes in model output with incremental changes in only $\delta_{\min}$, only K, or both $\delta_{\min}$ and K simultaneously. Second, sensitivity was explored on a broader scale at cells located across the spatial domain (n=655), examining the distributional change to larger modifications in $\delta_{\min}$ or K. The following sections discuss these analyses.

2.2.4.1. *Individual location analysis*

Simulations were run at six cells representing a range of climate conditions across eastern Sichuan Province (Figure 2.2). At each cell, a baseline time-series of snail density was obtained by running a single simulation with the parameter set from the fitting procedure (Section 2.2.3) that had the highest overall agreement with historical data and using the contemporary temperature dataset as model input. Next, using the same parameter set, $\delta_{\min}$ and K were modified by increasing and decreasing ($\pm$40%, in increments of 2%) the original value from the parameter set. Simulations were then run using these modified parameter sets, leading to a total of 1681 simulations per cell. For each simulation, mean snail density and day of first peak in snail density were examined, and their deviation from the baseline simulation was calculated.

2.2.4.2. *Distributional analysis*

To investigate how uncertainty in $\delta_{\min}$ and K affects predictions of future *O. hupensis* distribution, simulations were run using the future temperature dataset as input at a subset (n=655) of cells chosen at equal intervals across Sichuan Province, with the number of cells per county proportional to county size. For each simulation, the model was applied at every cell of the subset using the parameters sets estimated from the fitting procedure. Each simulation produced a daily snail density at every cell for the three years of simulation input. Daily snail density across the three years of simulation input was averaged to provide an estimate of

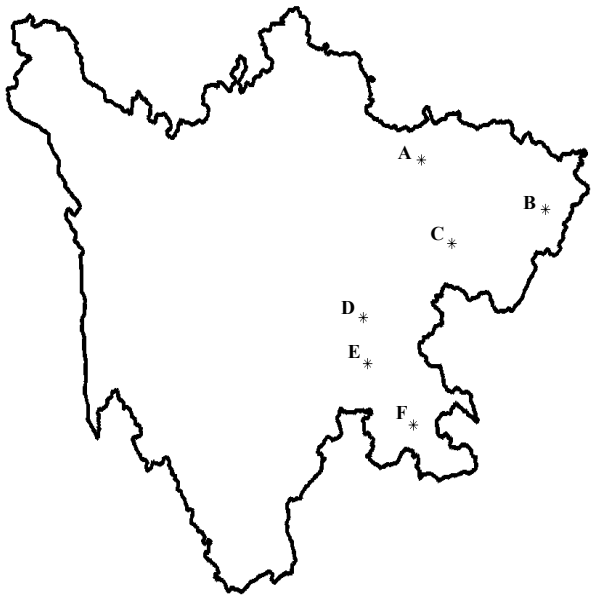

Figure 2.2: *Locations of the six cells chosen for the small-scale sensitivity analysis.*

mean snail density, and then averaged across all parameter sets. This process was repeated to generate a minimum snail density estimate at each cell for use in projecting regions of snail presence. The minimum snail density threshold, $s_{\min}$ (as described in Section 2.2.3), was used to define snail presence in projected distributions. To investigate the sensitivity of the results to this threshold, the analysis was repeated for several values of $s_{\min}$. Mean and minimum snail density values from the subset grid were spatially interpolated to yield values at all 90 x 90 meter cells across the spatial domain, yielding a baseline distribution and snail presence estimate for 2050. Finally, sensitivity to changes in $\delta_{\min}$ and K was investigated by increasing or decreasing the respective parameter in each set by 5%,

15%, 25%, or 35% and generating a new geographic distribution and snail presence estimate that was compared to the future baseline case.

All sensitivity analyses were conducted using MATLAB (version R2009a).

2.3. Results

2.3.1. *Temperature projection model*

The variables retained in the final model used to generate future temperature projections are shown in Table 2.3, along with model coefficients. When compared to the full model, which significantly and systematically over-predicted observed temperatures (Student's t, H_0:$(\text{pred-obs})_{\text{avg}} = 0$, $p < 0.00005$), the final (reduced) model did not significantly over- or under-predict station temperatures ($p = 0.72$). The mean difference between the observed mean monthly temperature and the model-predicted monthly temperature was 0.027 °C. What is more, when the final model was used to project the linear trend observed from 1980-2009 into future years, there was broad agreement with the IPCC predicted increase of 2.3–4.9°C by 2100 for the region (Solomon et al., 2007). Thus, the simple linear projections of the historic warming trend in Sichuan to 2050 were taken as a plausible future scenario for examining the influence of parametric uncertainty in degree-day models.

2.3.2. *Parameter estimation*

Among the density thresholds for "presence" explored, a threshold of $s_{\min} = 7$ snails per Kuang (a traditional Chinese sampling frame, equal to 0.11 m^2), yielded

the greatest number of parameter sets with the highest agreement with historical data, and thus this value was used. However, the simulated distribution of snail presence across Sichuan was approximately the same over a range of threshold values. While this minimum density threshold was found to be the best fit to historical presence/absence data, this does not imply that *O. hupensis* populations require this minimum density to persist.

From the 2000 simulations that were run, a total of 81 parameter sets met the first three criteria. Of these parameter sets, 8 were excluded for failing the fourth criteria. This yielded a total of 73 parameter sets that were used in subsequent analyses, with agreement between simulated and historical snail presence ranging from 50% to 63%, agreement between simulated and historical snail absence ranging from 61% to 73%, and total agreement between simulations and historical data ranging from 60% to 66%.

Figure 2.3 shows simulations for each of the 73 parameter sets at two representative locations, one marked as historical snail presence (left), and one as historical snail absence (right). Note that since the model was fit using a minimum density criteria and flexible agreement criteria, the observed variance in snail density is expected. Additionally, Figure 2.4 shows simulations for each parameter set using temperature data that was looped to generate twelve years of simulation input, indicating that model equilibrium is generally achieved within the first three years of the simulation.

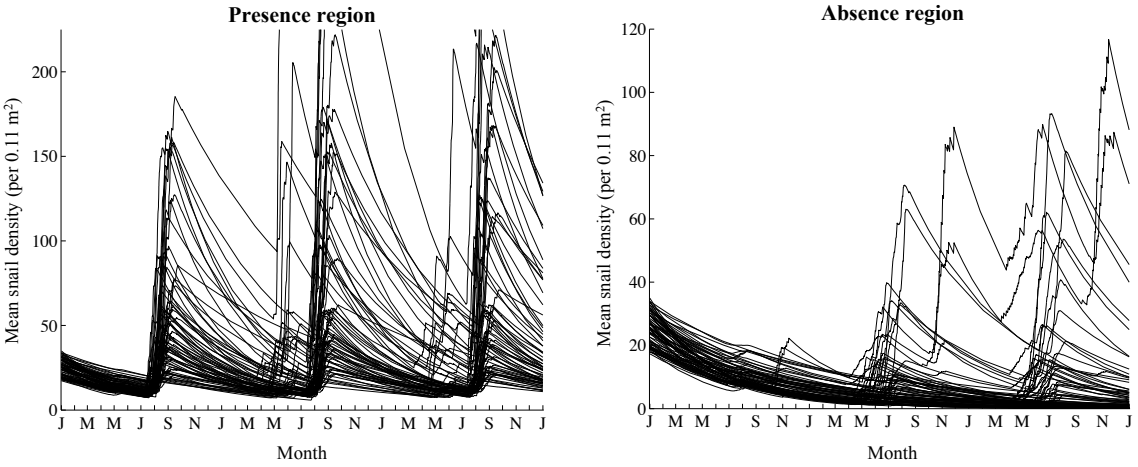

Figure 2.3: *Representative variation in model output (i.e. mean snail density) from the 73 parameter sets selected in the fitting procedure. Variation is shown at a cell fit to historical snail presence (left), and a cell fit to historical snail absence (right).*

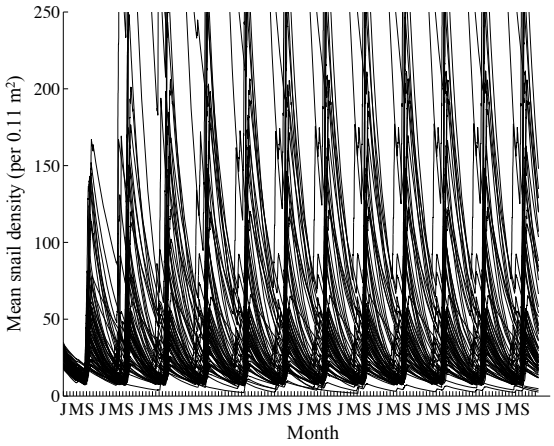

Figure 2.4: *Simulated mean snail density from all 73 parameter sets using twelve years of looped contemporary temperature data as input.*

2.3.3. *Sensitivity analysis*

2.3.3.1. *Individual cell analysis*

The sensitivity of model output at three representative cells (locations A, C, and D; see Figure 2.2) for the contemporary temperature dataset is shown in Figure 2.5, with plots showing the change in mean snail density and the first population

peak relative to the baseline simulation, given changes in $\delta_{\min}$ and K. Red colors indicate an increase in these outputs above the baseline value, while blue colors indicating a decrease below the baseline value. Results for locations B, E, and F exhibited similar patterns (data not shown). Decreases in $\delta_{\min}$ and/or K generally lead to increases in mean snail density and an earlier first population peak, and increases in $\delta_{\min}$ and/or K generally lead to decreases in mean snail density and a delayed first peak time. Note that the diagonal pattern observed in Figure 2.5 is due to the inverse relationship between $\delta_{\min}$ and K, a relationship that can be seen mathematically in Eqn. 2.1, and indicates a biological trade-off between these two parameters (Trudgill et al., 2005).

Often, the change in model output tends to be gradual, such as at locations C and D. However, in some regions even small changes in $\delta_{\min}$ and/or K can lead to large changes in model output. First instance, at location A, the baseline snail density using the contemporary dataset is 7.23 snails per 0.11 m^2, with the first population peak occurring in approximately July of the second year of the simulation. Decreasing either $\delta_{\min}$ or K by only 5% (such that $\delta_{\min}$ changes from 8.5 to 8.075 or K changes from 1440 to 1368) leads to a mean snail density of approximately 9.8 snails per 0.11 m^2 and the first population peak now occurring in November of the first year of the simulation. Even a change of 0.2% increases the mean snail density by approximately 24.5% and bumps the first population peak up to November of the first year (data not shown). Cells that exhibit the more gradual sensitivity to $\delta_{\min}$ and K appear to be in areas with temperatures that are often

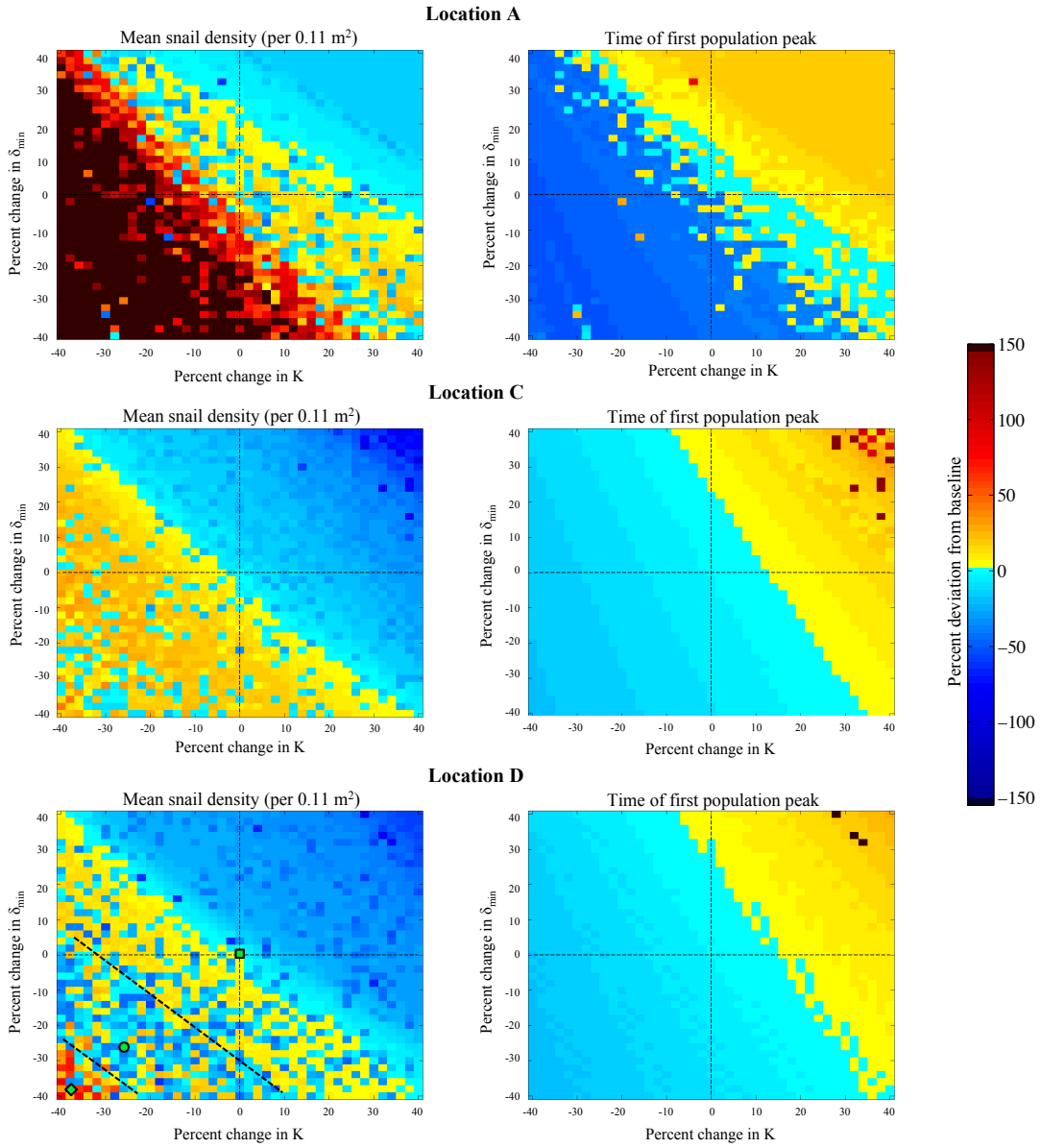

Figure 2.5: *Percent deviation from baseline simulation output (left column: mean snail density; right column: time of first population peak) given changes in* $\delta_{\min}$ *and* K *at three representative locations (Figure 2.2) within Sichuan Province. Red colors indicate a value greater than the baseline case, while blue colors indicate a value less than the baseline case. Baseline simulations were run using parameter values of* S_0*=22.642,* μ*=0.0049,* β*=0.4648,* α*=0.0195,* κ*=4.4672,* δ_{opt}*=23.08,* $\delta_{\min}$*=8.5, and* K*=1440. Percent changes in* $\delta_{\min}$ *and* K *are given along the y- and x-axes, respectively. Black lines in the plot of mean snail density at Location D (lower left) indicated the banding pattern observed (see text), while the green symbols in this same plot correspond to simulation output shown in Figure 2.7.*

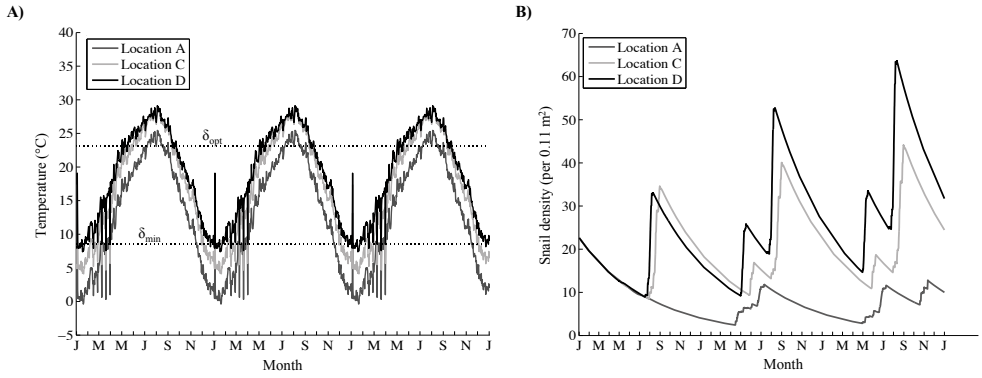

Figure 2.6: *A) Contemporary temperature data at Locations A (dark grey line), C (light grey line), and D (black line). B) Baseline simulation output at Locations A (dark grey line), C (light grey line), and D (black line), using parameter values of* S_0*=22.642,* μ*=0.0049,* β*=0.4648,* α*=0.0195,* κ*=4.4672,* δ_{opt}*=23.08,* δ_{min}*=8.5, and* K*=1440.*

close to or greater than the minimum temperature threshold (light grey and black lines, Figure 2.6A) and that exhibit stable population cycles (light grey and black lines, Figure 2.6B). Alternatively, cells that exhibit a strong sensitivity to δ_{min} and K appear to be those with temperature that often falls below the minimum threshold (grey line, Figure 2.6A) or that have unstable population cycles (i.e. exhibit an inconsistent number of population peaks per year; grey line, Figure 2.6B).

Mean snail density does not always increase strictly monotonically as δ_{min} and K decrease. Instead, in some cases the mean snail density initially increases as δ_{min} and K decrease, but then a region appears where the mean snail density is *less* than the baseline snail density, producing the banding pattern shown in the lower left corner of location D (Figure 2.5). As δ_{min} and K decrease further, the mean snail density is once again greater than the baseline value. To investigate this pattern further, simulation output at Location D was plotted using parameter values for

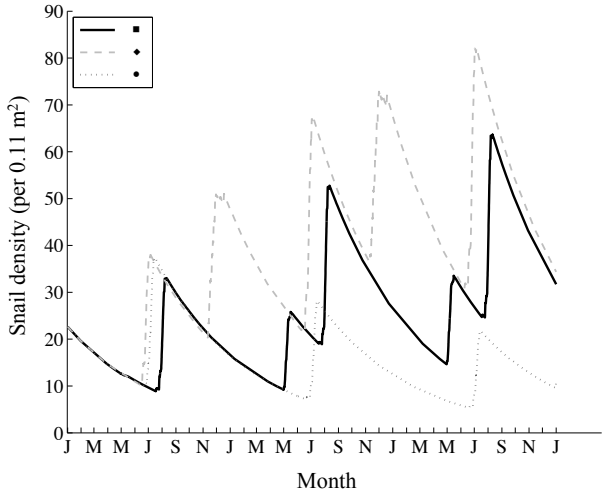

Figure 2.7: *Simulation output at Location D using the baseline parameter values (black line), and two modified parameter sets (grey lines). The first modified parameter set (dotted grey line) decreased both $\delta_{\min}$ and K by 26%, while the second modified parameter set (dashed grey line) decreased both $\delta_{\min}$ and K by 38%. Legend symbols corresponding to those found in Figure 2.5.*

$\delta_{\min}$ and K from each of these regions (green symbols, Figure 2.5) and then compared to the baseline simulation output (Figure 2.7). We see that, following the first year, the baseline population (solid line, Figure 2.7) experiences two population peaks per season, one in late spring–early summer, and the second in the fall. However, when the values of $\delta_{\min}$ and K fall within the range where the unexpected decrease in mean snail density was observed (dotted line, Figure 2.7), the seasonal peaks become disrupted as the timing of the completion of snail development no longer fully coincides with suitable temperature conditions. The small population peak observed early in the season is lost, and without this smaller peak to boost the population size, mean snail density decreases. As $\delta_{\min}$ and K both become much smaller than the baseline values (dashed line, Figure 2.7), the seasonal peaks are again disrupted. However, since $\delta_{\min}$ and K are now very small, population peaks

can occur even in the winter months, leading to two large peaks occurring at regular intervals throughout the year, and a subsequent increase in mean snail density.

2.3.3.2. *Distributional analysis*

The sensitivity of predicted mean snail density across Sichuan Province to changes in $\delta_{\min}$ and K is shown in Figure 2.8 for the 2050 temperature dataset. Comparable to the results at individual cells, mean snail density tends to increase as either $\delta_{\min}$ or K decreases, and tends to decrease as either $\delta_{\min}$ or K increases. Importantly, even a 5% change in $\delta_{\min}$ or K can lead to large changes in snail density, particularly around the edge of the snail distribution.

Additionally, the total area of snail presence (defined using a minimum snail density threshold of $s_{\min} = 5$, 6, 7, or 8 snails per 0.11 m^2) changes noticeably with changes in $\delta_{\min}$ or K (Table 2.4, Figure 2.9), particularly as either of these parameters increases. As $\delta_{\min}$ decreases by 35%, the total area of snail presence increases modestly by approximately 2%. A similar effect is observed when K decreases. However, as $\delta_{\min}$ or K increases up to 35%, the area of snail presence decreases, in some cases quite substantially. Using $s_{\min} = 7$, a 5% increase in $\delta_{\min}$ or K yields an approximately 56% and 42% decrease in area of snail presence, respectively (equivalent to a decrease of approximately 94,109 or 70,885 km^2 from the baseline area of 167,884 km^2). Interestingly, this dramatic decrease is much reduced as $\delta_{\min}$ or K are increased further. The large change in area of snail presence with small changes in $\delta_{\min}$ or K is not sensitive to the choice of $s_{\min}$ (Table

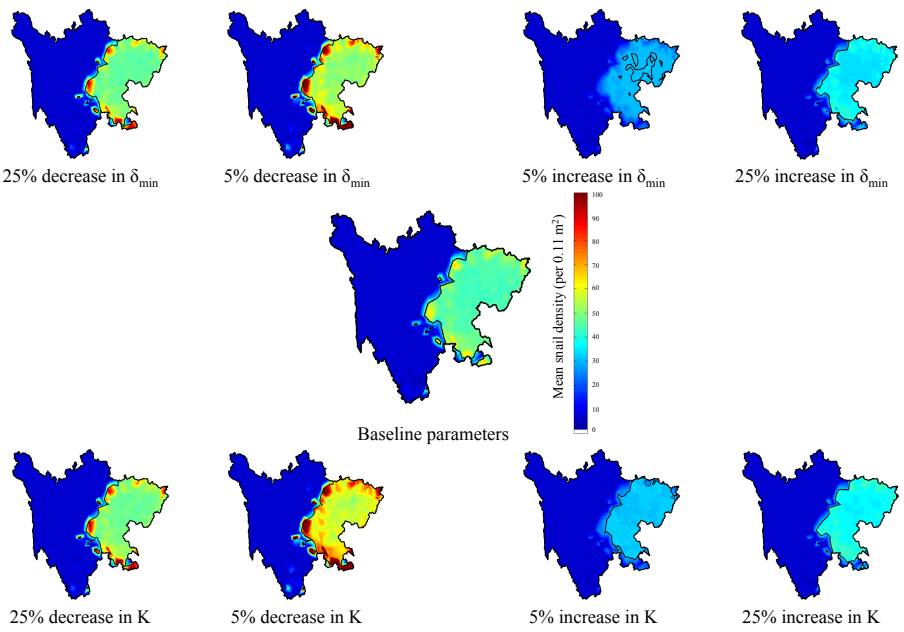

Figure 2.8: *Predicted mean snail density across Sichuan Province in 2050. Each plot represents the average snail density of the 73 parameter sets, with the center plot using the original parameter values, the top plots modifying* $\delta_{\min}$ *in each parameter set by the specified amount, and the bottom plots modifying* K *in each parameter set by the specified amount. Regions traced in black indicate areas of snail presence using a minimum snail density threshold of* $s_{\min} = 7$.

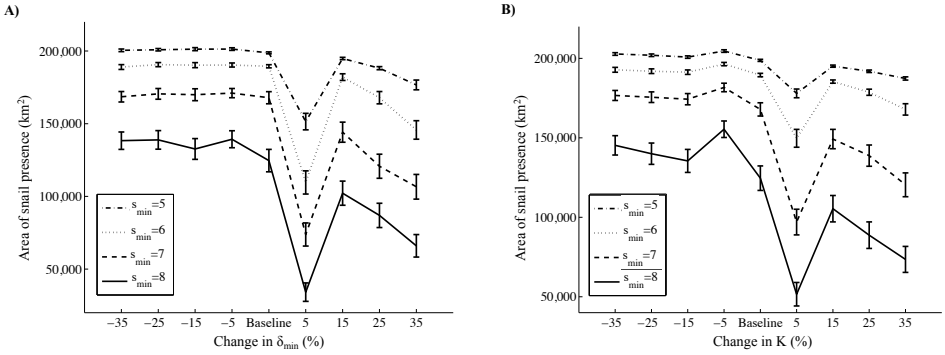

Figure 2.9: *Predicted mean area and standard error of snail presence in Sichuan Province in 2050 for* $s_{\min} = 5$ *(dotted-dashed lined),* $s_{\min} = 6$ *(dotted line),* $s_{\min} = 7$ *(dashed line), and* $s_{\min} = 8$ *(solid line). A) Predicted area given specified changes in* $\delta_{\min}$. *B) Predicted area given specified changes in* K.

2.4, Figure 2.9), although high $s_{\min}$ values tend to exhibit even greater sensitivity to changes in $\delta_{\min}$ or K.

Table 2.4: *Area of simulated snail presence given changes in $\delta_{\min}$ or K, with a minimum snail density threshold of $s_{\min} = 5$, $s_{\min} = 6$, $s_{\min} = 7$, or $s_{\min} = 8$. Values represent the mean of all 73 parameter sets, ± the standard error.*

Change in δ_{min} (%)	$s_{\min} = 5$ Area ± s.e. (km^2)	$s_{\min} = 6$ Area ± s.e. (km^2)	$s_{\min} = 7$ Area ± s.e. (km^2)	$s_{\min} = 8$ Area ± s.e. (km^2)
−35	200,478 ± 919	188,980 ± 1,639	168,534 ± 3,601	138,316 ± 6,001
−25	200,874 ± 841	190,630 ± 1,434	170,529 ± 3,705	138,858 ± 6,397
−15	201,272 ± 1,029	190,279 ± 1,722	169,932 ± 4,075	132,598 ± 7,151
−5	201,327 ± 887	190,364 ± 1,402	171,023 ± 3,166	139,308 ± 5,827
Baseline	**198,736 ± 653**	**189,507 ± 1,103**	**167,884 ± 4,173**	**124,614 ± 7,721**
5	151,454 ± 5,677	109,581 ± 7,986	73,775 ± 7,959	34,122 ± 6,353
15	194,830 ± 804	182,048 ± 2,306	144,161 ± 6,921	102,185 ± 8,306
25	188,193 ± 1,064	167,893 ± 4,233	120,732 ± 8,292	86,930 ± 8,347
35	176,676 ± 3,370	145,718 ± 6,365	106,611 ± 8,479	65,993 ± 7,743

Change in K (%)	$s_{\min} = 5$ Area ± s.e. (km^2)	$s_{\min} = 6$ Area ± s.e. (km^2)	$s_{\min} = 7$ Area ± s.e. (km^2)	$s_{\min} = 8$ Area ± s.e. (km^2)
−35	202,760 ± 837	192,815 ± 1,534	176,674 ± 3,150	145,285 ± 6,087
−25	201,953 ± 804	191,929 ± 1,484	175,564 ± 3,336	139,993 ± 6,711
−15	200,823 ± 765	191,303 ± 1,414	174,300 ± 3,538	135,474 ± 7,240
−5	204,612 ± 807	196,396 ± 1,046	181,682 ± 2,676	155,406 ± 5,176
Baseline	**198,736 ± 653**	**189,507 ± 1,103**	**167,884 ± 4,173**	**124,614 ± 7,721**
5	177,966 ± 2,741	149,699 ± 5,614	96,999 ± 8,067	51,578 ± 7,386
15	195,105 ± 667	185,398 ± 1,013	149,241 ± 6,095	105,390 ± 8,299
25	191,877 ± 784	178,677 ± 1,947	138,807 ± 6,696	88,751 ± 8,358
35	187,360 ± 1,011	167,894 ± 3,581	120,435 ± 7,505	73,502 ± 8,194

2.4. Discussion

Considerable uncertainty exists in key degree-day model parameters, and even modest uncertainty in a parameter can have a significant effect on model output. The analyses presented here show that the timing of peak population levels and the total area of snail presence are highly sensitive to even moderate changes in two parameters, the minimum temperature threshold of development, $\delta_{\min}$, and the total degree-days required for development to complete, K. Decreases in these two parameters generally cause simulated snail populations to exhibit higher mean snail densities and an earlier first peak in population size, while increases in these two parameters generally cause simulated snail populations to exhibit lower mean snail

densities and a delayed first peak in population size. Importantly, even changes as low as 0.2% can have a striking effect.

This result has important implications in the application of degree-day models, particularly for predictive forecasting. For instance, reliable predictions of peak population levels are necessary to inform vector or host control measures (e.g. predator release, pesticides, chemotherapies), since these measures are often timed to target specific organism densities or life stages. Estimated peak population dates that are off by several weeks or months could thus have severe consequences for the efficacy of timed intervention. In addition, the sensitivity to $\delta_{\min}$ and K is particularly pronounced in regions where snail populations are unstable, or where the yearly temperature profile often falls below or near the minimum temperature threshold. These regions are likely prevalent along the edges of the existing snail distribution, and as these regions are highly sensitive to errors in specifications of $\delta_{\min}$ and K, the uncertainty in a resulting map of organism distribution using the degree-day framework is particularly high. Identifying regions that could currently support vector or host populations, or that might support vector or host populations under future climate change conditions, is necessary for effective disease monitoring and for the planning of control and treatment options. If identified regions are inaccurate, decisions on where to conduct vector or host control or monitoring activities now, or in the future, will be misinformed.

Another interesting result that emerges from incorporating the degree-day model into a dynamical population model is the disruption of seasonality that can

occur given changes in $\delta_{\min}$ and K. In some cases, a decrease in either of these parameters will lead to a shift toward a population peak earlier in the season, enabling the population to peak twice per year. This additional peak could lead to increases in disease risk, and thus increase the need for control and monitoring activities. In other cases, this shift in the timing of the population peaks disrupts the population cycling, leading to dampening, single peaks over the three year simulation. This predicted decrease in snail density may imply a reduced risk of transmission, or might indicate that control methods being conducted are effective. However, since all three results (declining snail density, one peak per season, and two peaks per season) can be generated by uncertainty in $\delta_{\min}$ and K, it seems clear that in order for control measures to be effectively implemented, this uncertainty needs to be better understood and accounted for.

In addition, parametric uncertainty is only one of several factors to be considered when applying degree-day models (Chapter 1). Of particular concern is the assumption of a linear relationship between the rate of development and temperature (Kontodimas et al., 2004). Although this assumption simplifies the model and increases its ease of use, insect development is often non-linear (Beck, 1983), exhibiting an exponential increase in the rate of development up to an optimal temperature, followed by a declining rate above the optimal temperature. Portions of the nonlinear response curve can be represented linearly; however, this approximation is only accurate within a limited range of temperatures (Bonhomme, 2000). Thus, the application of these models is constrained to temperature ranges

that fall within the bounds for which the model was parameterized. In changing environments, or when applied to questions of climate change, temperatures may shift outside the range for which the degree-day model can be reliably applied.

Though not incorporated in the analyses above, other factors such as additional environmental variables (e.g. precipitation, humidity, vegetation, etc.), anthropogenic effects, and uncertainties associated with estimating future temperatures (Bergant et al., 2006) should also be considered when making statements of organism distribution in response to changing climates.

2.5. Conclusion

Care should be used when applying degree-day models to make predictions of organism distribution and dynamics under scenarios of climate change. Model output is highly sensitive to changes in model parameters, and thus parametric uncertainty should always be considered when applying degree-day models. Researchers should consider conducting their own sensitivity analysis with regard to model parameters when reporting results; at the very least, the potential impact of model uncertainty on specific conclusions and recommendations should always be discussed. Additionally, degree-day models are valid only at intermediate temperature ranges for which the linear approximation is accurate, and thus, if the temperature often falls at or beyond the extremes of organism development, an alternate model should be considered. However, with these cautions in mind, the

degree-day model shows promise for applications to ecological responses to climate change, and can be a useful tool for studying temperature-dependent development.

2.6. Acknowledgements

I would like to thank Song Liang for providing the historical snail data and developing the original population model, Adam Akullian for obtaining and interpolating the Sichuan temperature data, and Nina Townsend for developing and validating the statistical model used to project the Sichuan temperature data.

Conclusion

In this thesis I examined the structural and parametric issues related to the application of degree-day models, specifically to study the response of organisms to a changing climate. I found that model specifications are important to consider in the context of the specific organism and region under study, as different model specifications (i.e. the choice of a functional response, temperature threshold cutoffs, and degree-day calculation methods) can lead to substantially different results. Additionally, I found that degree-day model results are highly sensitive to uncertainty in model parameters, and that this uncertainty should be accounted for when applying these models. I conclude that, given the limitations and assumptions of the degree-day model, their use should be restricted to scenarios for which the assumptions hold, and used cautiously in studies of climate change. However, when used within these bounds, the degree-day model can be an insightful tool for studying temperature-dependent development.

Bibliography

P.G. Allsopp and D.G. Butler. Estimating day-degrees from daily maximum-minimum temperatures: A comparison of techniques for a soil-dwelling insect. *Agr. Forest Meteorol.*, 41(1-2):165–172, 1987.

S.D. Beck. Insect thermoperiodism. *Annu. Rev. Entomol.*, 28(1):91–108, 1983.

J.C. Beier. Malaria parasite development in mosquitoes. *Annu. Rev. Entomol.*, 43 (1):519–543, 1998.

F. Bensadia, S. Boudreault, J.F. Guay, D. Michaud, and C. Cloutier. Aphid clonal resistance to a parasitoid fails under heat stress. *J. Insect Physiol.*, 52(2):146–157, 2006.

K. Bergant and S. Trdan. How reliable are thermal constants for insect development when estimated from laboratory experiments? *Entomol. Exp. Appl.*, 120:251–256, 2006.

K. Bergant, L.K. Bogataj, and S.E. Travers. Uncertainties in modelling of climate change impact in future: An example of onion thrips (*Thrips Tabaci* Lindeman) in Slovenia. *Ecol. Model.*, 194:244–255, 2006.

R. Bonhomme. Bases and limits to using degree day units. *Eur. J. Agron.*, 13:1–10, 2000.

P.M. Brakefield and V. Mazzotta. Matching field and laboratory environments: effects of neglecting daily temperature variation on insect reaction norms. *J.*

Evolution. Biol., 8(5):559–573, 1995.

J.F. Briere, P. Pracros, A.Y. le Roux, and J.S. Pierre. A novel rate model of temperature-dependent development for arthropods. *Environ. Entomol.*, 28(1): 22–29, 1999.

O. Buyukalaca, H. Bulut, and T. Yilmaz. Analysis of variable-base heating and cooling degree-days for Turkey. *Appl. Energ.*, 69(4):269–283, 2001.

A. Campbell, B.D. Frazer, N. Gilbert, A.P. Gutierrez, and M. Mackauer. Temperature requirements of some aphids and their parasites. *J. Appl. Ecol.*, 11 (2):431–438, 1974.

C. Cesaraccio, S. Donatella, P. Duce, and R.L. Snyder. An improved model for determining degree-day values from daily temperature data. *Int. J. Biometeorol.*, 45:161–169, 2001.

M. Christenson, H. Manz, and D. Gyalistras. Climate warming impact on degree-days and building energy demand in Switzerland. *Energy Convers. Manage.*, 47(6):671–686, 2006.

Z. Chuanyan, N. Zhongren, and C. Guodong. Methods for modelling of temporal and spatial distribution of air temperature at landscape scale in the southern Qilian mountains, China. *Ecol. Model.*, 189(1-2):209–220, 2005.

J.C. Corley and O.A. Bruzzone. Delayed emergence and the success of parasitoids in biological control. *Biol. Control*, 51(3):471–474, 2009.

M.H. Craig, R.W. Snow, and D. le Sueur. A climate-based distribution model of malaria transmission in sub-Saharan Africa. *Parasitol. Today*, 15(3):7, 1999.

G.R. Dabbs. Caution! All data are not created equal: The hazards of using National Weather Service data for calculating accumulated degree days. *Forensic. Sci. Int.*, 202(1-3):e49–e52, 2010.

D.L. Dahlsten, D.L. Rowney, and S.M. Tait. Development of integrated pest management programs in urban forests: the elm beetle (*Xanthogaleruca luteola* (Müller)) in California, USA. *Forest Ecol. Manag.*, 65(1):31–44, 1994.

H.V. Danks. Short life cycles in insects and mites. *Can. Entomol.*, 138:407–463, 2006.

J.C. Diaz-Perez. Root zone temperature, plant growth and yield of broccili [*Brassica oleracea* (Plench) var. *italica*] as affected by plastic film mulches. *Scientia Horticulturae*, 123:156–163, 2009.

ECAD. European Climate Assessment and Dataset, European Climate Support Network, 2011. URL `http://eca.knmi.nl/`. Accessed April 2011.

R.H. Elliott, L. Mann, and O. Olfert. Calendar and degree-day requirements for emergence of adult wheat midge, *Sitodiplosis mosellana* (Géhin) (Diptera: Cecidomyiidae) in Saskatchewan, Canada. *Crop Prot.*, 28(7):588–594, 2009.

D.W. Hagstrum and G.A. Milliken. Quantitative analysis of temperature, moisture, and diet factors affecting insect development. *Ann. Entomol. Soc. Am.*, 81: 539–546, 1988.

D.W. Hilbert and J.A. Logan. Empirical-model of nymphal development for the migratory grasshopper, *Melanoplus-sanguinipes* (Orthoptera, Acrididae). *Environ. Entomol.*, 12(1):1–5, 1983.

P.D. Hughes and R.J. Braithwaite. Application of a degree-day model to reconstruct Pleistocene glacial climates. *Quaternary Res.*, 69(1):110–116, 2008.

G.F. Killeen, F.E. McKenzie, B.D. Foy, C. Schieffelin, P.F. Billingsley, and J.C. Beier. A simplified model for predicting malaria entomologic inoculation rates based on entomologic and parasitologic parameters relevant to control. *Am. J. Trop. Med. Hyg.*, 62(5):535–544, 2000.

A.M. Kilpatrick, D.M. Fonseca, G.D. Ebel, M.R. Reddy, and L.D. Kramer. Spatial and temporal variation in vector competence of *Culex pipiens* and *Cx. restuans* mosquitoes for West Nile Virus. *Am. J. Trop. Med. Hyg.*, 83(3):607–613, 2010.

J.G. Kingsolver. Weather and the population dynamics of insects: Integrating physiological and population ecology. *Physiol. Zool.*, 62(2):314–334, 1989.

D.C. Kontodimas, P.A. Eliopoulos, G.J. Stathas, and L.P Economou. Comparative temperature-dependent development of *Nephus includens* and *Nephus bisignatus* preying on *Planococcus citri*: Evaluation of a linear and various nonlinear models using specific criteria. *Environ. Entomol.*, 33(1):1–11, 2004.

D.J. Lactin, N.J. Holliday, D.L. Johnson, and R. Craigen. Improved rate model of temperature-dependent development by arthropods. *Environ. Entomol.*, 24:68–75, 1995.

F. Lardeux and J. Cheffort. Temperature thresholds and statistical modelling of larval *Wuchereria bancrofti* (Filariidea: Onchocercidae) developmental rates. *Parasitology*, 114:123–134, 1997.

S. Liang, D. Maszle, and R.C. Spear. A quantitative framework for a multi-group model of *Schistosomiasis japonicum* transmission dynamics and control in Sichuan, China. *Acta Trop.*, 82:263–277, 2002.

S. Liang, R.C. Spear, E. Seto, A. Hubbard, and D. Qiu. A multi-group model of *Schistosoma japonicum* transmission dynamics and control: model calibration and control prediction. *Trop. Med. Int. Health*, 10(3):263–278, 2005.

S. Lindsay, D. Hole, R. Hutchinson, S. Richards, and S. Willis. Assessing the future threat from vivax malaria in the United Kingdom using two markedly different modelling approaches. *Malaria J.*, 9(1):1–8, 2010.

J.A. Logan and J.A. Powell. Ghost forests, global warming, and the mountain pine beetle (Coleoptera: Scolytidae). *Am. Entomol.*, 47:160–173, 2001.

J.A. Logan, D.J. Wollkind, S.C. Hoyt, and L.K. Tanigoshi. Analytic model for description of temperature-dependent rate phenomena in arthropods. *Environ. Entomol.*, 5(6):1133–1140, 1976.

J.D. Logan. An index to measure the effects of temperature change on trophic interactions. *J. Theor. Biol.*, 246:366–376, 2007.

J.D. Logan, W. Wolesensky, and A. Joern. Insect development under predation risk, variable temperature, and variable food quality. *Math. Biosci. Eng.*, 4(1):47–65, 2007.

C. Lopez, A. Sans, L. Asin, and M. EizaGuirre. Phenological model for *Sesamia nonagrioides* (Lepidoptera: Noctuidae). *Environ. Entomol.*, 30(1):23–30, 2001.

G.S. McMaster and W.W. Wilhelm. Growing degree-days: one equation, two interpretations. *Agr. Forest Meteorol.*, 87:291–300, 1997.

Ministry of Health. *Epidemiological Situation of Schistosomiasis in China in 1989*. Chengdu University of Science and Technology Press, 1992.

H.F. Nahrung, M.K. Schutze, A.R. Clarke, M.P. Duffy, E.A. Dunlop, and S.A. Lawson. Thermal requirements, field mortality and population phenology modelling of *Paropsis atomaria* Olivier, an emergent pest in subtropical hardwood plantations. *Forest Ecol. Manag.*, 255(8-9):3515–3523, 2008.

P. Naves and E. de Sousa. Threshold temperatures and degree-day estimates for development of post-dormancy larvae of *Monochamus galloprovincialis* (Coleoptera: Cerambycidae). *J. Pest. Sci.*, 82(1):1–6, 2009.

P. Nieto, J.B. Malone, and M.E. Bavia. Ecological niche modeling for visceral leishmaniasis in the state of Bahia, Brazil, using genetic algorithm for rule-set prediction and growing degree day-water budget analysis. *Geospatial Health*, 1(1): 115–126, 2006.

NOAA. US Climate Reference Network, 2011. URL `http://www.ncdc.noaa.gov/crn/`. Accessed April 25, 2011.

J.J. Obrycki and T.J. Kring. Predaceous Coccinellidae in biological control. *Annu. Rev. Entomol.*, 43(1):295–321, 1998.

N.H. Ogden, M. Bigras-Poulin, C.J. O'Callaghan, I.K. Barker, L.R. Lindsay, A. Maarouf, K.E. Smoyer-Tomic, D. Waltner-Toews, and D. Charron. A dynamic population model to investigate effects of climate on geographic range and

seasonality of the tick *Ixodes scapularis*. *Int. J. Parasitol.*, 35:375–289, 2005.

N.H. Ogden, A. Maarouf, I.K. Barker, M. Bigras-Poulin, L.R. Lindsay, M.G. Morshed, C.J. O'Callaghan, F. Ramay, D. Waltner-Toews, and D. Charron. Climate change and the potential for range expansion of the lyme disease vector of *Ixodes scapularis* in Canada. *Int. J. Parasitol.*, 36:63–70, 2006.

K.P. Paaijmans, A.F. Read, and M.B Thomas. Understanding the link between malaria risk and climate. *P. Natl. Acad. Sci.*, 106(33):13844–13849, 2009.

K.P. Paaijmans, S. Blanford, A.S. Bell, J.I. Blanford, A.F. Read, and M.B. Thomas. Influence of climate on malaria transmission depends on daily temperature variation. *P. Natl. Acad. Sci.*, 107(34):15135–15139, 2010a.

K.P. Paaijmans, S. Imbahale, M. Thomas, and W. Takken. Relevant microclimate for determining the development rate of malaria mosquitoes and possible implications of climate change. *Malaria J.*, 9(196):1–8, 2010b.

J.A. Powell and J.A. Logan. Insect seasonality: circle map analysis of temperature-driven life cycles. *Theor. Popul. Biol.*, 67(3):161–179, 2005.

X. Qian. *Atlas of Schistosomiasis in China*. China Atlas Society, 1987.

R.A. Reaumur. Observations du thermometre faites pendant l'annee 1735 comparees a celles qui ont ete faites sous la ligne a l'isle-de-france, a alger et en quelques-unes de nos isles de l'amerique. *Memoires de l'Academie Royale des Sciences*, pages 545–576, 1735.

D.C. Reicosky, L.J. Winkelman, J.M. Baker, and D.G. Baker. Accuracy of hourly air temperatures calculated from daily minima and maxima. *Agr. Forest*

Meteorol., 46(3):193–209, 1989.

J. Remais, A. Hubbard, W.U. Zisong, and R.C. Spear. Weather-driven dynamics of an intermediate host: mechanistic and statistical population modelling of *Oncomelania hupensis*. *J. Appl. Ecol.*, 44(4):781–791, 2007.

C.Z. Ren, B.L. Ma, V. Burrows, J. Zhou, Y.G. Hu, L. Guo, L. Wei, L. Sha, and L. Deng. Evaluation of early mature naked oat varieties as a summer-seeded crop in dryland northern climate regions. *Field Crop Res.*, 103(3):248–254, 2007.

W.J. Roltsch, F.G. Zalom, A.J. Strawn, J.F. Strand, and M.J. Pitcairn. Evaluation of several degree-day estimation methods in California climates. *Int. J. Biometeorol.*, 42(4):169–176, 1999.

A.G.P. Ross, A.C. Sleigh, Y.S. Li, G.M. Davis, G.M. Williams, Z. Jiang, Z. Feng, and D.P. McManus. Schistosomiasis in the People's Republic of China: Prospects and challenges for the 21st century. *Clin. Microbiol. Rev.*, 14(2):270–295, 2001.

M. Roy, J. Brodeur, and C. Cloutier. Relationship between temperature and developmental rate of *Stethorus punctillum* (Coleoptera : Coccinellidae) and its prey *Tetranychus mcdanieli* (Acarina : Tetranychidae). *Environ. Entomol.*, 31(1): 177–187, 2002.

M.J. Samways. Climate diagrams and biological control: An example from the areography of the ladybird *Chilocorus nigritus* (Fabricius, 1798) (Insecta, Coleoptera, Coccinellidae). *J. Biogeogr.*, 16(4):345–351, 1989.

I. Sanchez-Ramos and P. Castanera. Development and survival of *Tyrophagus putrescentiae* (Acari : Acaridae) at constant temperatures. *Environ. Entomol.*, 30

(6):1082–1089, 2001.

A. Semadeni-Davies. Monthly snowmelt modelling for large-scale climate change studies using the degree day approach. *Ecol. Model.*, 101(2-3):303–323, 1997.

P.J.H. Sharpe and D.W. DeMichele. Reaction-kinetics of poikilotherm development. *J. Theor. Biol.*, 64(4):649–670, 1977.

B.S. Sharratt, C.C. Sheaffer, and D.G. Baker. Base temperature for the application of the growing-degree-day model to field-grown alfalfa. *Field Crop Res.*, 21(2): 95–102, 1989.

R.L. Snyder, D. Spano, C. Cesaraccio, and P. Duce. Determining degree-day thresholds from field observations. *Int. J. Biometeorol.*, 42(4):177–182, 1999.

S. Solomon, D. Qin, M. Manning, Z. Chen, M. Marquis, K.B. Averyt, M. Tignor, and H.L Miller. Contribution of Working Group I to the Fourth Assessment Report of the Intergovernmental Panel on Climate Change, 2007. Technical report, 2007.

P. Thakur, S. Kumar, J.A. Malik, J.D. Berger, and H. Nayyar. Cold stress effects on reproductive development in grain crops: An overview. *Environ. Exp. Bot.*, 67 (3):429–443, 2010.

P.C. Tobin, S. Nagarkatti, and M.C. Saunders. Modeling development in grape berry moth (Lepidoptera : Tortricidae). *Environ. Entomol.*, 30(4):692–699, 2001.

D.L. Trudgill, A. Honek, D. Li, and N.M. Van Straalen. Thermal time – concepts and utility. *Ann. Appl. Biol.*, 146(1):1–14, 2005.

A.F. Tzikopoulos, M.C. Karatza, and J.A. Paravantis. Modeling energy efficiency of bioclimatic buildings. *Energ. Buildings*, 37(5):529–544, 2005.

Integrated Pest Management Program University of California. Run models and calculate degree-days, 2011a. URL `http://www.ipm.ucdavis.edu/WEATHER/ddretrieve.html`. Accessed May 19, 2011.

Integrated Pest Management Program University of California. Degree-days, 2011b. URL `http://www.ipm.ucdavis.edu/WEATHER/ddconcepts.html#Degree-dayconcepts`. Accessed May 19, 2011.

Prairie Research Institute University of Illinois. Daily pest degree-day accumulations, 2011. URL `http://www.isws.illinois.edu/warm/pestdata/`. Accessed May 19.

Extension Ag Weather University of Wisconsin. Degree day calculator, 2011. URL `http://www.soils.wisc.edu/uwex_agwx/thermal_models/degree_days`. Accessed May 19, 2011.

M.E. Visser and C. Both. Shifts in phenology due to global climate change: the need for a yardstick. *P. Roy. Soc. Lond. B. Bio.*, 272(1581):2561–2569, 2005.

L.-D. Wang, J.-G. Guo, X.-H. Wu, H.-G. Chen, T.-P. Wang, S.-P. Zhu, Z.-H. Zhang, P. Steinmann, G.-J Yang, S.-P. Wang, Z.-D. Wu, L.-Y. Wang, Y. Hao, R. Bergquist, J. Utzinger, and X.-N. Zhou. Chinas new strategy to block *Schistosoma japonicum* transmission: experiences and impact beyond

schistosomiasis. *Trop. Med. Int. Health*, 14(12):1475–1483, 2009.

L.T. Wilson and W.W. Barnett. Degree-days: an aid in crop and pest management. *California Agriculture*, pages 4–7, January-February 1983.

G.J. Yang, A. Gemperli, P. Vounatsou, M. Tanner, X.N. Zhou, and J. Utzinger. A growing degree-day based time-series analysis for prediction of *Schistosomiasis japonicum* transmission in Jiangsu Province, China. *Am. J. Trop. Med. Hyg.*, 75 (3):549–555, 2006.

G.J. Yang, Q. Gao, S.S. Zhou, J.B. Malone, J.C. McCarroll, M. Tanner, P. Vounatsou, R. Bergquist, J. Utzinger, and X.N. Zhou. Mapping and predicting malaria transmission in the People's Republic of China, using integrated biology-driven and statistical models. *Geospatial Health*, 5(1):11–22, 2010.

S. Yang, J. Logan, and D.L. Coffey. Mathematical formulae for calculating the base temperature for growing degree days. *Agr. Forest Meteorol.*, 74(1-2):61–74, 1995.

Z. Zhang, S.H. Ong, W. Peng, Y. Zhou, J. Zhuang, G. Zhao, and Q. Jiang. A model for the prediction of *Oncomelania hupensis* in the lake and marshland regions, China. *Parasitol. Int.*, 57(2):121–131, 2008.

X.N. Zhou, J.G. Guo, X.H. Wu, Q.W. Jiang, J. Zheng, H. Dang, X.H. Wang, J. Xu, H.Q. Zhu, G.L. Wu, Y.S. Li, X.J. Xu, H.G. Chen, T.P. Wang, Y.C. Zhu, D.C. Qiu, X.Q. Dong, G.M. Zhao, S.J. Zhang, N.Q. Zhao, G. Xia, L.Y. Wang, S.Q. Zhang, D.D. Lin, M.G. Chen, and Y. Hao. Epidemiology of schistosomiasis in the People's Republic of China, 2004. *Emerg. Infect. Dis.*, 13(10):1470–1476, 2007.

X.N. Zhou, G.J. Yang, X.H. Wang, Q.B. Hong, L.P. Sun, J.B. Malone, T.K. Kristensen, N.R. Bergquist, and J. Utzinger. Potential impact of climate change on schistosomiasis transmission in China. *Am. J. Trop. Med. Hyg.*, 78(2):7, 2008.

L. Zou, S.N. Miller, and E.T. Schmidtmann. A GIS tool to estimate west nile virus risk based on a degree-day model. *Environ. Monit. Assess.*, 129(1-3):413–420, 2007.